EXPERIMENTS IN NEUTRON PRODUCTION.

An abstract of a thesis submitted for the degree of Doctor of Philosophy to the Board of the Faculty of Physical Sciences in the University of Oxford.

Trinity Term,
1949.

P.C. Thonemann,
Trinity College,
Oxford.

MS. D. Phil. d. 752

Dep. i. SD

ABSTRACT.

A precise method of monitoring the neutron yield from the D-D reaction would provide a convenient standard source of fast monokinetic neutrons. The possible reactions are :

$$D^2 + D^2 \rightarrow He^3 + n^1 + 3.18 \text{ M.V.}$$
$$\rightarrow H^3 + H^1 + 3.98 \text{ M.V.}$$

In principle this objective could be achieved by counting the number of He^3 nuclei emitted in a known solid angle. Because of their short range, however, (4.3 mm. in air) it is more convenient to monitor the 14.7 cm. range protons and the neutron flux is then determined if the ratio of the two reaction is known as a function of bombarding energy. The branching ratio is also of theoretical interest. The determination of the ratio of the yield in the two reactions was the objective in the experiments described.

Existing ion sources were not considered capable of fulfilling the necessary requirements of reliability, high deuteron percentage and small energy inhomogeneity, and the first half of the investigation was devoted to developing an ion source which would satisfy the above requirements.

Observations by Hertzberg* on the Balmer spectrum emitted in an electrodeless ring discharge suggested a means of producing an ionized gas from which it should be possible to obtain a high percentage of atomic ions. An ion source was developed using this method of excitation.

The factors effecting the concentration of atomic gas are investigated in detail, and a theory of atomic hydrogen recombination on metal and glass surfaces is put forward which fits the experimental observations. In addition the mechanism of ionization by electron collision in hydrogen is reviewed and its relationship to proton percentage and energy inhomogeneity in the final proton beam is pointed out.

It is shown theoretically that the maximum ion beam current which can be extracted from the discharge and focussed through a canal is determined by space charge repulsion in the beam. The limiting current is determined by the canal dimensions and the maximum gas flow which can be tolerated. The theoretical expression for the case of a proton beam is :

$$I_{max} = 3.79 \times 10^{-6} V^{3/2} R^2/L^2 \text{ amperes.}$$

V = probe potential in volts.

R = canal radius

L = canal length.

To approach this limiting current it is necessary to extract ions from a curved plasma boundary. The focussing produced by various electrode arrangements was investigated photographically, and an efficient design evolved.

After leaving the canal the beam divergies under its own space charge. The rate of divergence is calculated so that a focussing lens can be designed to accept the full beam.

A Nier mass spectrograph of the 90° deflection type was

built to investigate the atomic and molecular ion percentages. It was necessary to stabilize the magnetic field to 1 part in 5000 and the accelerating potential to 1 part in 2000 in order to estimate the proton energy spread in the beam. The resolving power was 1 part in 250 (mass units).

The performance of a typical ion source is summarized in the table.

Radio frequency power input at 20 megacycles	200 watts.
Gas pressure	0.02 mm. of Hg.
Probe current	7 mA.
Probe voltage	4 K.V.
Proton percentage	80%
Total beam current	1 mA.
Gas leak	15 cc/hour
Energy inhomogeneity	90% of protons have an energy spread of less than ± 20 volts.

The ion source was fitted to a 300 K.V. accelerator in which the power for the discharge, the probe voltage and palladium leak was supplied by transmitting radio frequency power at three different frequencies up a condenser transmission line. No difficulty was experienced in focussing a 300 micro-ampere deuteron beam on the target.

Initial experiments on the D-D reaction were designed to investigate the degree of separation of the particle groups recorded in a proportional counter. A twin channel pulse amplitude selector was built for this purpose. Because of the

small range of the He^3 nuclei (4.3 mm. in air) some difficulty was experienced in making a window which would admit this particle to the counter without excessive energy loss. A thin window of silica proved finally to be the most satisfactory.

It was found impossible to adequately separate the three particle groups in a single counter. At high pressures (10 cm. of Hg.) the He^3 group merged into the H^3 group, and at low pressures (3 cm. of Hg.) scattered deuterons completely obscured the H^1 peak, although resolution of the He^3 and H^3 groups was excellent. This difficulty was removed by using twin counters separated by a thin aluminium foil. The first counter recorded the H^3 and He^3 nuclei, and the second the protons. Both counters were operated in the proportional region to reduce spurious counts due to gamma rays. At 82 and 111 K.V. scattered deuterons were observed entering the first counter but did not prevent almost complete resolution of the H^3 peak. At 139 K.V. scattered deuterons made resolution of the H^3 group on the low energy side impossible, and measurements of the branching ratio depend only on the He^3 and H^1 counts.

The He^3/H^3 ratio is obtained by plotting a bias curve and using the heights of the two plateaux, the proton counter being used only as a monitor. The H^3/H^1 ratio is determined directly from the position of the He^3 plateau. Because of the incomplete resolution both plateaux should show a small slope which because of statistical counting errors is not observed. The slope of the plateau is estimated from the contours obtained with the

vi

pulse amplitude selector, and a correction of +1% added to the final branching ratio. Excellent agreement is obtained for the branching ratio computed separately from the He^3/H^1 ratio and the He^3/H^3 ratio. The final results are set out in the table :

82 ± 5 K.V.		111 ± 5 K.V.		139 ± 10K.V
He^3/H^1	He^3/H^3	He^3/H^1	He^3/H^3	He^3/H^1
0.80 ± .02	0.88 ± .06	0.90 ± .04	0.87 ± .07	1.11 ± .05
0.87 ± .03	0.86 ± .05	0.89 ± .02	0.85 ± .03	1.09 ± .05
0.87 ± .03	0.84 ± .05	0.89 ± .02	1.03 ± .03	
0.89 ± .03	0.84 ± .04	0.91 ± .03	0.98 ± .06	
0.84 ± .03	0.82 ± .09	0.93 ± .02	1.07 ± .02	
Mean		Mean		
0.85 ± .03		0.93 ± .06		
correction for plateau slope + 0.01		correction for plateau slope + 0.01		Final Result
Final Result		Final Result		
0.86 ± .04		0.94 ± .07		1.11 ± .0

Based on the measurements of the cross-section for proton production in the D-D reaction at 182 K.V. by Bretscher, French and Seidl* the cross-section for neutron production at 90° to the incident beam is 1.45×10^{-26} cm^2 with an error of ± 10%.

* Phys.Rev. 73, 815, 1948.

EXPERIMENTS IN NEUTRON PRODUCTION.

A thesis submitted for the degree of Doctor of Philosophy to the Board of the Faculty of Physical Sciences in the University of Oxford.

P.C. Thonemann,
Trinity College,
Oxford.

Trinity Term,
1949.

Summary.

The development of a radio frequency ion source for use with high voltage accelerators is described. A mass spectrograph of the Nier type, built for the purpose, was used to investigate the proton percentage and homogeneity of the ions under a wide range of conditions. After 50 K.V. acceleration and analysis, deuteron currents of 400 microamps have been obtained. The source has proved very stable in operation.

Using this ion source on a 300 K.V. accelerator a direct determination of the ratio of the yield from the two reactions

$$D^2 + D^2 \rightarrow He^3 + n^1$$
$$\rightarrow H^3 + H^1$$

at 90° to the incident beam, has been made, by counting protons, tritons and helium nuclei in two proportional counters filled with Argon (90%) and Alcohol at 6 cm. pressure. The helium and tritons are recorded by the first counter and protons by the second. An aluminium window 0.0005" thick prevented helium and tritons entering the second counter.

A pulse amplitude selector was built for identifying the particle groups and to find the optimum counter pressures for the best resolution. Complete separation of the particle groups was not achieved due to interference from scattered deuterons and gamma ray background. However, the ratio determined firstly by He^3/H^1 and secondarily by He^3/H^3 agreed within the statistical counting errors. For incident deuteron energies of 139 K.V. scattered deuterons interfered with the

resolution of the H^3 peak and the ratio was then computed from He^3/H^1 counts. The results are :

Deuteron energy	82 ± 5 K.V.	111 ± 5 K.V.	139 ± 10 K.V.
Ratio He^3/H^1	0.86 ± 0.4	0.94 ± .07	1.11 ± .08

The absolute cross section for neutron production σ_{dn} is computed from the results of Bretscher, French and Seidl (61) using their cross section for the (d,p) reaction and angular distribution function.

Deuteron energy.	82 ± 5 K.V.	111 ± 5 K.V.	139 ± 10 K.V
σ_{dn} cm^2 ± 10%	1.45×10^{-26}	2.14×10^{-26}	3.42×10^{-26}

CONTENTS.

Page.

Introduction.

1. Ion Source Development (Theoretical).

Section.

1-1 Ionization processes in hydrogen 1

1-2 The production of atomic hydrogen gas 3

1-3 The extraction of positive ions from a plasma 6

1-4 Space charge limitation of ion currents in a cylindrical canal 10

1-5 Focussing of positive ions into the canal 13

1-6 Focussing of the ion beam 15

2. Ion Source Development (Experimental).

2-1 Ion focussing by curved plasma boundary 16

2-2 The use of constant magnetic field to increase the ion density above the probe 17

2-3 Spectroscopic investigations of discharge 18

2-4 Suppression of secondary electrons from probe 19

2-5 Mass spectrograph for beam analysis 20

2-6 Effect of H_2O and O_2 on proton percentage 21

2-7 The influence of a constant magnetic field on proton percentage 23

2-8 Final ion source design and performance 24

2-9 Variation of proton percentage with R.F. power input 29

2-10 Variation of proton percentage with gas pressure 31

2-11 Energy inhomogeneity of deuteron atomic ions 32

2-12 Conclusion 33

Page.

3. Experimental determination of the D-D branching ratio.

3-1 Introduction 34

3-2 Preparation of the counter windows 35

3-3 Relative pulse amplitude due to H^1, H^3 and He^3 nuclei 36

3-4 Preliminary experiments 38

3-5 Description of pulse amplitude selector 40

3-6 Description of linear amplifiers 42

3-7 Description of twin counter arrangement 43

3-8 Loss of particles by the Rutherford scattering in the silica window 45

3-9 Background due to neutron recoil nuclei 46

3-10 Background due to gamma rays 46

3-11 Method of measurement 47

3-12 Discussion of results 50

3-13 The absolute cross section for the $D(D,n)He^3$ reaction 52

3-14 Discussion on theory 53

3-15 Conclusion 57

Acknowledgements 58

Appendix I 59

Appendix II 61

References 63

ION SOURCE DEVELOPMENT.

Introduction.

Although a multitude of different kinds of ion sources have been described in the literature, the continued publication of new types and modifications show that older models have not proved entirely satisfactory. This position is largely due to the fact that many aspects of gas discharges are still in the state of an art rather than a science.

The hot cathode type of source which is favoured in America suffers from a disadvantage that frequent replacements of the cathode are necessary, whilst the cold cathode type gives ions whose energy is spread over a wide range. The high frequency discharge appears to offer a possible solution to both these difficulties.

Without an understanding, however, of the fundamental processes of ionization, and the mode in which ions can be extracted from an ionized gas, little improvement over existing types can be expected. The investigations described are an attempt to analyse the most important factors in ion source design and an attempt is made to apply these principles to the construction of a more satisfactory source.

1. Ion Source Development (Theoretical).

1-1 Ionization processes in hydrogen.

Ion sources may be classified into two general types, those in which ions are extracted from a plasma or region of intense ionization (Ref. 1,2,3,4,5) and those in which the ions are formed in a region where the electrical field strength may be tens of volts/cm. (6,7). The ion beams produced by the first type would be expected to have energy inhomogeneities not greater than a few tens of volts since the electrode potential differences employed are usually less than 200 volts whilst the second group employ potential differences up to 50 K.V. and have inhomogeneities of the same magnitude.

In principle, therefore, it is possible to obtain a much larger ion current of well defined energy, after analysis, if the initial energy spread of the ions is small. An additional factor which favours the low voltage ion source is the possibility of achieving a high proton percentage; it is of interest, therefore, to consider electron collision processes in hydrogen for energies less than 200 electron volts.

Table I. Ionization processes by electron collision in hydrogen.

	Reaction.	Minimum electron energy (e.v.)	Energy for maximum cross-section (e.v.)	Reference.
1.	$H_2 \rightarrow H_1 + H_1 + 7$ e.v.	11.5	15	(8)
2.	$H_2 \rightarrow H_2^+$	15.9	70	(10)
3.	$H_1 \rightarrow H_1^+$	13.5	70	(9)
4.	$H_2 \rightarrow H_1 + H_1^+$	18.0	-	(10)
5.	$H_2 \rightarrow H_1 + H_1^+ +$ K.E.	28.0	-	(10)
6.	$H_2 \rightarrow H_1^+ + H_1^+ +$ K.E.	46.0	-	(10)

In addition positive ions can make the following transitions:

		Reference.
7.	H_2^+ (fast) + H_2 (slow) $\rightarrow$ $H_1^+ + H_1 + H_2^+$ (slow)	(11)(12)
8.	H_2^+ (fast) + H_2 (slow) $\rightarrow$ H_2 (fast) + H_2^+ (slow)	(13)
9.	H_2^+ (slow) + H_2 (slow) $\rightarrow$ $H_3^+ + H_1$ + 1.7 e.V.	(14)
10.	H_3^+ (fast) + H_2 (slow) $\rightarrow$ H_1^+ (fast) + H_2 (fast) + H_2 (slow)	(11)(12)

Proton percentages exceeding 50% have been attained in two ways. (a) By bombarding the molecular gas with electrons of high energy so that reactions 4, 5 and 6, have a total cross-section comparable with 2, and by allowing the molecular ions to travel through the neutral gas at a comparatively high pressure (approximately 0.1 mm.) so that reactions 7 and 10 contribute to the proton current in the beam. The cross-sections for these latter reactions have not been measured so that no quantitative estimate of their importance can be made.

(b) By producing a high concentration of atomic gas according to reaction 1. The primary positive ions formed are predominantly H_1^+. The dissociation of hydrogen molecules by electron impact has been discussed theoretically by Mott and Massey (8) and demonstrated experimentally by Hughes and Skellet (15), Glocker, Baxter and Dalton (16) and Whiddington and Jones (17). The production of atomic hydrogen gas is discussed fully in section 1-2. In the analysis of ion beams from all sources is found H_3^+. Recent computations (14) of the binding energy of H_3^+ indicate that the reaction 9 is exothermic by about 1.7 e.V. and is, therefore, the most probable mode of H_3^+ formation. H_3 is unstable against dissociation into H_2 and H_1 (14).

A reduction of the partial pressure of H_2 by dissociation leads, therefore, to less rapid production of H_3^+. This is an additional reason for favouring atomic rather than molecular hydrogen in the discharge tube.

1-2 <u>The production of atomic hydrogen gas</u>.

Dissociation of H_2 by electron collision results from excitation into the lowest triplet state. This state is unstable for electron spins both parallel and anti-parallel (18). The resulting neutral atoms separate with a mutual kinetic energy equal to the difference between the energy of the unstable triplet state (11.5 e.V.) and the dissociation energy (4.5 e.V.). Calculations (19) indicate that the

dissociation cross-section rises to a maximum, comparable with the elastic cross-section, a few volts above the critical potential, and falls off very rapidly with increasing velocity of impact. Evidence for the existence of a strong 9 volts energy loss for electrons of energies between 14 and 26 volts in hydrogen have been obtained by Whiddington and Jones (17).

To achieve any useful concentration of atomic gas it is necessary that recombination into molecular hydrogen should be a minimum. Volume recombination requires the simultaneous collision of two hydrogen atoms and another particle, and this process can be minimized by working at low gas pressures.

Hertzberg (20) using an electrodeless ring discharge in a glass tube whose inner walls were coated with a layer of ice, was able to photograph some 20 lines of the Balmer series. To accomplish this the partial pressure of the molecular gas must be exceedingly low otherwise molecular band spectra masks the higher series lines. A number of other workers (21,22,23,24) have been successful in producing atomic hydrogen gas in high concentrations, and it is observed that whilst metal surfaces are very efficient in causing recombination glasses are much less effective.

The following discussion is an attempt to explain the results of Wood and Hertzberg.

Recombination of atomic hydrogen to the molecular form is a radiationless process requiring the presence of a third body (no electronic energy levels below 11.5 e.V.).

At pressures above 1 mm. appreciable volume recombination may take place by three body collisions but below this pressure recombination on the walls of the tubes and electrodes is predominant.

If a metal is introduced into the gas atomic hydrogen reduces any oxide which may be present and a surface hydride is formed (25,26). It is known (27) that strong surface forces corresponding to unsaturated valency bonds exist at a clean metallic surface, moreover absorbed impurity atoms are mobile. The bond energy of hydrogen on metal surfaces is estimated (28) to be approximately 2 e.V. so that two hydrogen atoms approaching close enough can form a molecule and escape as a neutral molecule, the difference between the dissociation energy and the atom-metal bonds being communicated to the metal.

For materials whose oxides are not readily reducible (SiO_2, AL_2O_3) surface oxygen saturates the valency bonds and an incident hydrogen atom is not captured. After prolonged exposure to atomic hydrogen, however, even these materials are reduced at the surface to the metallic state and recombination occurs. On this basis ice is the ideal material for the inner walls of a tube. The O-H bond is stronger than the H-H bond and provided the incident H atom has insufficient kinetic energy to break the O-H bond it must rebound. When the mean free path of the H atom becomes comparable with the dimensions of the vessel they may hit the surface with a kinetic energy of 3.5 e.V. In addition the electron temperature of a low pressure discharge

is high and a rapid decomposition of surface oxides is to be expected by electron bombardment. There exists, therefore, a pressure at which volume recombination is negligible and the mean free path of the hydrogen atoms is small compared to the vessel dimensions. At this pressure the atomic hydrogen concentration is expected to be a maximum.

1-3 The extraction of positive ions from a plasma.

If two electrodes at different potentials are immersed in a plasma, almost the entire potential difference is confined to a region surrounding the negative electrode. This behaviour is a consequence of the high mobility of the electrons compared to the positive ions.

The collection of positive ions by a negative electrode was first investigated by Langmuir and his collaborators (29,30, 31) in a low pressure mercury arc discharge. They measured visually the depth of the dark sheath surrounding the probe and found agreement with that calculated from Child's space charge equation. The positive ion current density was calculated from random rate of drift of positive ions, temperature T_2, across the sheath boundary. The observed current densities required, however, positive ion temperature of the order 10,000°K. Langmuir, later, abandoned this explanation based on the Schottky ambipolar diffusion theory (34,35) and investigated in great detail the mode of ambipolar drift to the tube walls (32) for the case of $\lambda \gg r$. This theory was verified by

Killian (33) using a low pressure mercury arc. Langmuir and Tonks' theory in a slightly different form may be applied to the collection of ions by a negative probe. The original incorrect methods still appear in the great majority of text books on the gas discharges. Although the quantitative application of this theory to ion sources is unmanageable because of the complicated electric field surrounding the probe electrode, some general conclusions can be drawn from it.

In a high frequency electrodeless discharge at low pressure the ions and electrons generated in gas recombine on the walls of the vessel. The positive ions are accelerated by a radial electric field which at the same time diminishes the drift velocities of the electrons so as to maintain a zero nett radial flow of charge. In the absence of collision ($\lambda \gg r$) this electric field alone determines the drift velocity of the positive ions and the random thermal velocities make a negligible contribution. To compute the positive ion current to a negative probe it is necessary to know how far the field of the probe extends into the plasma and then to calculate the rate of production of positive ions within this volume. The positive ion current depends, therefore, on :

(a) T_1, the electron temperature,

(b) n_1, the electron concentration,

(c) n_o, the neutral gas concentration,

(d) Z, the number of ion pairs formed per electron per unit time.

Calculations are complicated by the additional electric

fields which maintain ambipolar drift to the non-conducting walls of the vessel. The surface of the volume from which ions are drawn to the probe is in fact limited only be the presence of these additional electrical fields. The shape and dimensions of the vessel containing the ionized gas must, therefore, play an important part in determining the ion current to the probe.

Since the ions are produced in regions of different potential their energies will not be the same at the probe surface. In a retarding field the concentration of electrons is given by the Boltzmann relation :

$$n_1 = n_{1,0}\, e^{-\frac{eV}{kT_1}}$$

The rate of production of ions is proportional to the electron concentration and 90% of the ions are formed in a region over which the variation of potential is given by :

$$e^{-\frac{eV}{kT_1}} = 1/10 \quad \text{i.e.} \quad \text{e.V.} = 2.3\ kT_1$$

At a pressure of 0.02 mm. and a tube diameter of 4 cms. the electron temperature in molecular hydrogen calculated on data given by v. Engel and Steenbeck (36) is 1.6×10^5°K. i.e. e.V. = 31.5 electron volts. No figures are available for computing the electron temperature in atomic hydrogen, but the energy inhomogeneity in this case must certainly be of the same order of magnitude.

If the depth of field penetration is comparable with the mean free path of the ions, ~~th~~ inelastic collisions may increase the energy spread. The number of ion pairs produced per cm.

per mm. Hg. for protons in molecular hydrogen (37) is very small for energies below 2000 e.V., and it is doubtful whether excitation or ionization would contribute appreciably to the energy inhomogeneity of the positive ions.

Because of charge exchange a considerable proportion of ions extracted from the plasma are lost. Assuming a cross-section comparable with the kinetic theory cross-section (38) the free path for charge exchange at the above pressure is approximately 1 cm. The visual depth of the sheath above a probe in the ion source is about 4 mm. and some 10% of the ions leaving the plasma are neutralized on their way to the probe. However, since the free path for re-ionization, at energies up to 5 K.V., is very long compared to 4 mm., no contribution to the energy inhomogeneity can come from this source.

If an appreciable percentage of molecular hydrogen is present high speed protons can be produced by the reactions :

$$H_2 \rightarrow H_1^+ + H^+ + K.E., \qquad H_2 \rightarrow H_1^+ + H_1 + K.E.$$

Due to the coulomb repulsion between the two nuclei the protons separate with an energy of approximately 8 e.V. The percentage of H_2^+ measured in the final ion source is not more than 10%. At electron temperature of the order 10^5°K. the reaction $H_2 \rightarrow H_2^+$ is undoubtedly more probable than either of the above, and no appreciable energy spread can be attributed to these reactions.

It is concluded that the main energy inhomogeneity is due to the formation of ions in regions of different potential.

1-4 Space charge limitation of ion currents in a cylindrical canal.

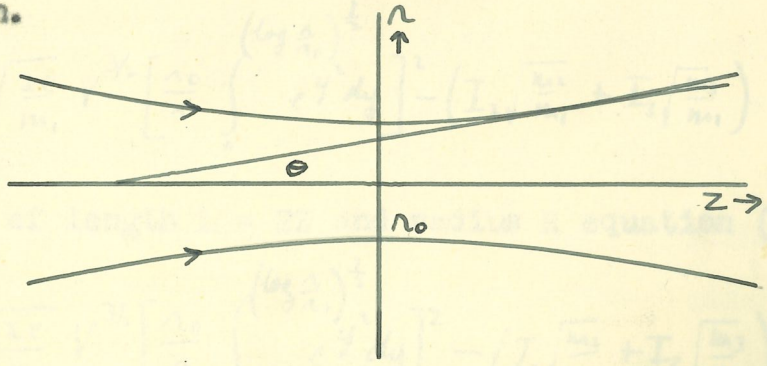
Due to the radial electrical field produced by the ions, an initially parallel beam diverges. The current of ions passing through a cylindrical canal is limited by this divergence. To calculate this limiting current the following assumptions are made :

(a) The cross-section of the beam is everywhere circular and the ion density has circular symetry.

(b) An ion initially on the beam boundary remains on the boundary.

(c) All ions have the same longitudinal velocity.

The last assumption imposes the restriction that the angle of divergence of the beam is small. For beams having a divergence greater than $>5^{\circ}$ the calculated results are only correct to a first approximation.



Consider a beam of ions, each of charge e, which converges to a minimum diameter r_0 at z = 0 and θ the angle, the tangent to the beam envelope, makes with the z axis. The equation of

motion of an ion of mass m on the boundary is :

$$d^2r/dz^2 = eE/m\dot{z}^2 = E/2V \qquad \ldots.(1)$$

where E. is the radial electric field and V is the potential through which the ions have been accelerated. It follows from equation (1) that the curvature of the beam is independent of the ion mass so that no separation of mass species occurs.

If the current density of ions of mass m, is I_1, m_2 is I_2 and m_z is I_3 then E is given by :

$$E = z/r(I_1/\dot{z}_1 + I_2/\dot{z}_2 + I_3/\dot{z}_3) \qquad \ldots\ldots.(2)$$

and $d^2/r/dz^2 = 1/V(I_1/z_1 + I_2/z_2 + I_3/z_3)$ $\ldots\ldots.(3)$

With the boundary conditions dr/dz = 0, Z = 0 when r = r_o, the solution of (3) is : (see Appendix I)

$$I_1 = \frac{2r^2}{Z^2}\sqrt{\frac{2e}{m_1}}V^{3/2}\left[\frac{r_0}{r}\int_0^{\left(\log\frac{r}{r_0}\right)^{\frac{1}{2}}} e^{y^2}dy\right]^2 - \left(I_2\sqrt{\frac{m_2}{m_1}} + I_3\sqrt{\frac{m_3}{m_1}}\right) \qquad \ldots..(4)$$

For a canal of length L = 2Z and radius R equation (4) becomes :

$$I_1 = \frac{8R^2}{L^2}\sqrt{\frac{2e}{m_1}}V^{3/2}\left[\frac{r_0}{r}\int_0^{\left(\log\frac{r}{r_0}\right)^{\frac{1}{2}}} e^{y^2}dy\right]^2 - \left(I_2\sqrt{\frac{m_2}{m_1}} + I_3\sqrt{\frac{m_3}{m_1}}\right) \ldots.(5)$$

A maximum current can pass through the canal for a value of r_o given by :

$$\frac{d}{dr_0}\left(r_0\int_0^{\left(\log\frac{R}{r_0}\right)^{\frac{1}{2}}} e^{y^2}dy\right) \qquad \ldots.(6)$$

This condition is satisfied by $R = 2.33\, r_0$, i.e. $(\log R/r_0)^{\frac{1}{2}} = 0.920$.

Equation (5) becomes :

$$(I_1)_{max} = 2\cdot34 \frac{R^2}{L^2}\sqrt{\frac{2e}{m_1}}V^{3/2} - \left(I_2\sqrt{\frac{m_2}{m_1}} + I_3\sqrt{\frac{m_3}{m_1}}\right) \quad \ldots.(7)$$

With V in volts, I in amperes, m = proton mass equation (7) becomes :

$$(I_1)_{max.} = 3\cdot79\times10^{-6}\frac{R^2}{L^2}V^{3/2} - \left(I_2\sqrt{\frac{m_2}{m_1}} + I_3\sqrt{\frac{m_3}{m_1}}\right) \quad \ldots.(8)$$

From this equation it follows that :

$$(\tan\theta)_{r\,=\,2.33\,r_0} = 2R/L \quad \ldots.(9)$$

Thus the maximum current flows through the canal when the tangent to the beam envelope at the point of entry and exit passes through the origin.

These results may be applied without modification to the flow in a conducting canal provided the beam axis coincides with the canal axis. In the absence of symmetry image fields in the conductor tend to deflect the beam towards the walls.

The presence of heavy ions in the beam can greatly reduce the proton current I_1 by contributing to the space charge spreading and thus the maximum current which may pass through the canal.

The equation for the envelope of the maximum current beam is found by substituting $(I_1)_{max}$ for I_1 in equation (5) giving

$$Z = \pm\, 0\cdot923\,\frac{L}{R}\,r_0\int_0^{\left(\log\frac{2\cdot33\,r}{R}\right)^{\frac{1}{2}}} e^{y^2}\,dy \quad \ldots.(10)$$

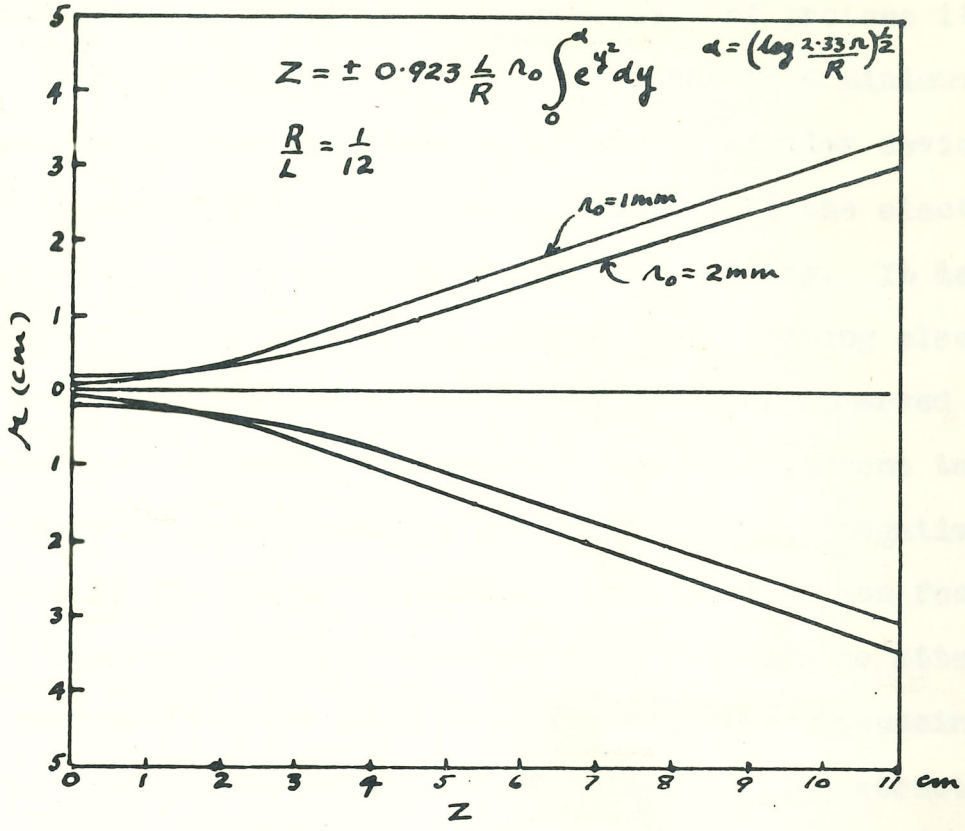


Figure I. The theoretical envelope of the maximum current beam for two values of the minimum radius r_0.

The envelope has been plotted (Figure I) for the case R/L = 1/12 and r_0 = 1 mm. and 2 mm. The rate of expansion of the beam increases with decreasing r_0.

1-5 Focussing of positive ions into the canal.

The focussing of electrons by a curved emitting surface has been studied by Pierce (42), Samuels (43), and Field (44), and it has been demonstrated by Thonemann (45) that the same principle may be applied to ions extracted from a curved

plasma boundary. To obtain a high percentage of protons it is important to reduce the exposed metal surfaces to a minimum. In the absence of this restriction an exactly similar device to that used by Pierce (42) would serve, except that the electron emitting surface is replaced by the plasma boundary. It is possible, however, to replace the Pierce field forming electrode with a glass surface since an insulating material immersed in a plasma takes up a potential which makes the nett current to it zero. This potential is usually two or three volts negative with respect to the plasma potential. This mode of ion focussing has been used in the present investigation although no attempt has been made to find the best shape for the glass focussing structure. A closer investigation of this focussing structure is necessary if ion current approaching the theoretical limits are to be attained.

The centre of curvature of the plasma boundary must lie at the canal centre and the shape of the glass focussing structure so arranged that the ions follow radial paths to the canal centre. The semi-angle subtended by the plasma boundary at the centre of the canal is then given by $\tan\theta = 2R/L$ and the boundary ions enter the canal along a diagonal. The position of the an ion beam on the axis of the canal is one of unstable equilibrium. A small radial displacement of the beam gives rise to image fields which tend to deflect it to the walls. In the early experiments in which the canal was in a field free space this unstability made it almost impossible to pass the ions through

a canal. Additional focussing fields at the entrance of the canal are necessary to give the beam radial stability.

1-6 Focussing of the ion beam.

The divergent ion beam leaving the canal may be focussed by the methods familiar in electron optics. The only difference being the increased importance of space charge. Space charge spreading with magnetic focussing appears to be negligible due to the accumulation of electrons in the beam (39,40).

The following considerations have guided the design of electrostatic focussing systems :

(a) The angle ϕ subtended by the lens radius at the canal is given by $\tan 2\phi = 2R/L$. This implies that the beam fills half the geometrical lens diameter.

(b) Electrical breakdown across the lens set a limit to the "aperture" of the lens.

(c) The focal length of the lens must be chosen so as not to produce excessive magnification of the image. Data given by Terman (41) have proved reliable.

For maximum beam current the image seen by the lens extends from the centre of the lens to a point Z_o given approximately

$$Z_o = Z_1 - 3.03\, r_1 \qquad \ldots.(11)$$

where r_1, Z_1 are the coordinates of an ion on the boundary of the beam at the lens centre. Values of (Z_1, r_2) may be found from Figure I. For Z_1 = 10 cm., r_1 = 2.7 cm. and Z_o = 1.9 cm. The image found by the lens has then strong

spherical aberration, the boundary ions being focussed some distance behind the axial ions. Spherical aberration in the lens tends to correct this aberration.

2. Ion source development. (Experimental).

2-1 Ion focussing by curved plasma boundary.

A 60 megacycle 500 watt oscillator of conventional design, using a CV.29 tube was built for the excitation of the discharge. The luminosity of the discharge was always greatest when excited by a resonant inductance coiled around the tube (electrodeless ring discharge (20,46)). The circulating electron currents were evidently of the same order as those in the coil as the discharge produced considerable detuning of the resonant circuit. This type of discharge was used in all subsequent experiments.

The focussing of the ions extracted from a curved plasma boundary was investigated visually and photographically in a large scale ion source (H_2 pressure 0.005 mm.) using a gauze cylinder to represent a canal. The heat dissipation due to secondary electrons striking the anode made it necessary to use oil cooling. This experiment using the ring discharge showed the same focussing phenomena as the earlier electrostatic method of excitation (45). After operation for some hours a conducting film was deposited on the neck of the vessel and destroyed the focussing mechanism thus illustrating the importance of surface charges on the glass.

The position of minimum beam diameter did not change

appreciably with probe voltage variations although the actual diameter of focus could be reduced to a few millimetres at the highest extracting voltage (6-7 K.V.). When the beam was focussed to its minimum diameter a strong diffuse luminosity in the neighbourhood of the focus suggested that secondary ionization was taking place. In addition strong sputtering of the brass gauze occurred even though the direct beam was focussed along the axis. The radial space charge field of the beam is certainly sufficient to accelerate electrons, liberated from the gauze, to energies high enough to produce additional ionization and excitation.

Attempts to pass the beam through an aluminium canal (4 mm. diameter, 20 mm. long) were only partially successful. The beam moved around the canal edges but could only be passed through with difficulty. It was pointed out in section 1-5 that such an unstability could be expected when the point of entry of the beam was in a field free space. Later experiments showed that strong radial focussing field are necessary if the beam is to be held on the axis of the canal.

2-2 <u>The use of constant magnetic fields to increase the ion density above the probe.</u>

If the electrode containing the canal is to be used for extracting the ions from the plasma its diameter is limited by the available pumping speeds. A high ion density is therefore necessary immediately above the probe.

A new tube was constructed in which a tungsten anode was isolated by a constriction from the discharge space. The aluminium extracting electrode contained the canal. The radial component of the electric field between the probe and the plasma might be expected to give the ion beam radial stability. No further difficulty was experienced in aligning the ion beam and the canal with this arrangement. A conical shaped iron pole piece was used to support the probe and by means of a coil wound around the ion a convergent magnetic field (1000 gauss at pale top) could be used to concentrate the discharge over the probe.

For a fixed R.F. power input the magnetic field produced a strong increase in luminosity immediately above the probe and probe current and ion beam current were much greater than previously. However, the same conditions could be reproduced by increasing the R.F. power input and probe currents far in excess of those which could be conveniently supplied in an accelerator ion source were readily obtainable without the magnetic field. No further investigations were carried out with this type of magnetic field.

2-3 Spectroscopic investigation of discharge.

In principle it should be possible to estimate the concentration of atomic gas by spectroscopic methods. The complexity of the calculations however make this possibility of little practical value. Eleven lines of the Balmer series

could be counted on plates taken with a small Hilger quartz spectrograph. When an impurity gas is present and the discharge colour is bluish-white instead of red only three lines were observed. The molecular band spectra masks the higher lines of the series.

Measurements with the mass spectrograph showed that the proton percentage dropped from about 80% to 20% when the discharge colour changed from red to white.

2-4 Suppression of secondary electron emission from probe.

In some early experiments secondary electrons emitted from the probe melted a hole through the glass envelope and an attempt was made to reduce this secondary current.

By painting the probe canal with magnesium oxide, incandescence indicated the regions of positive ion bombardment. The ions extracted from the plasma could be focussed through the canal entrance but a brilliant incandescence was observed near the base of the canal. Secondary electrons from this region are guided back up the canal by the radial space charge field of the positive ions. To suppress these electrons a new type of probe with an insulated canal was used (Figure 2).

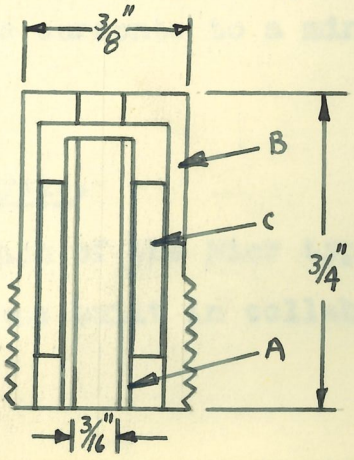


Figure 2.
Probe for suppression
of secondary electrons.

An aluminium tube A was insulated from the main body of the probe B by the ceramic C. The potential of tube A could be varied relative to B. The results are tabulated in Table 2.

Potential of A. (volts).	Current to A. (ma).	Target current (secondaries not suppressed).	B Current (ma).
+ 400	- 5 (electron collection)	1.0 ma.	3
300	- 2	1.0	3
200	0	1.5	5
100	5.5	2.0	12.5
0	12.0	2.0	20
Floating	0	1.5	5

The results demonstrate that the major current of the secondary electrons is emitted from within the canal and the total probe current, with the insulated section floating was only one quarter of its value with the canal connected to the probe body.

In the final design the probe diameter was reduced to 0.25" and the canal to 0.125" and no excessive heating of the glass envelope by secondaries has been observed. However, if it is necessary to restrict the probe currents to a minimum the composite probe is an advantage.

2-5 Mass spectrograph for beam analysis.

A 90° deflection mass spectrograph of the Nier type with a maximum resolving power $\frac{\Delta m}{m} = 1/250$ was built in collaboration

with Messrs. J.H. Sanders and J. Moffatt. The electrical circuits were adapted from those published by Graham and Thode (47) with the exception of the stabilized 10 K.V. supply designed by J. Moffatt. A high resolving power was necessary to measure the proton energy inhomogeneity. Figure 3 is a block diagram of the arrangement. Ions extracted from the discharge were focussed on the 0.1 mm. slit S1. Slit S3 prevented destruction of S1 by the beam. A third slit S4 collimated the ions to a 2.5^{0} beam. The receiving slit S2 was made ≅1. mm. wide for percentage measurements. The radius of curvature of the beam in the magnetic field was 5 cm. The magnetic field was stable to 1 part in 5000 and the high tension supply to 1 part in 2000. The slits could be aligned with the apparatus in operation.

It was found impossible to take measurements of ion current as a function of magnetic field strength because of bad hysteresis in the electromagnet. A small 0-300 volts power supply was connected in series with the main high tension supply and ion current contours were plotted against high tension voltage for a fixed magnetic field. Bypass condensers reduced radio frequency interference to less than 2 volts R.M.S. For homogeneity measurements a Faraday screen surrounded the ion source envelope as it is possible that the alternating electrostatic field from the exciting coil could contribute to the ion inhomogeneity.

2-6 Effect of H_2O and O_2 on proton percentage.

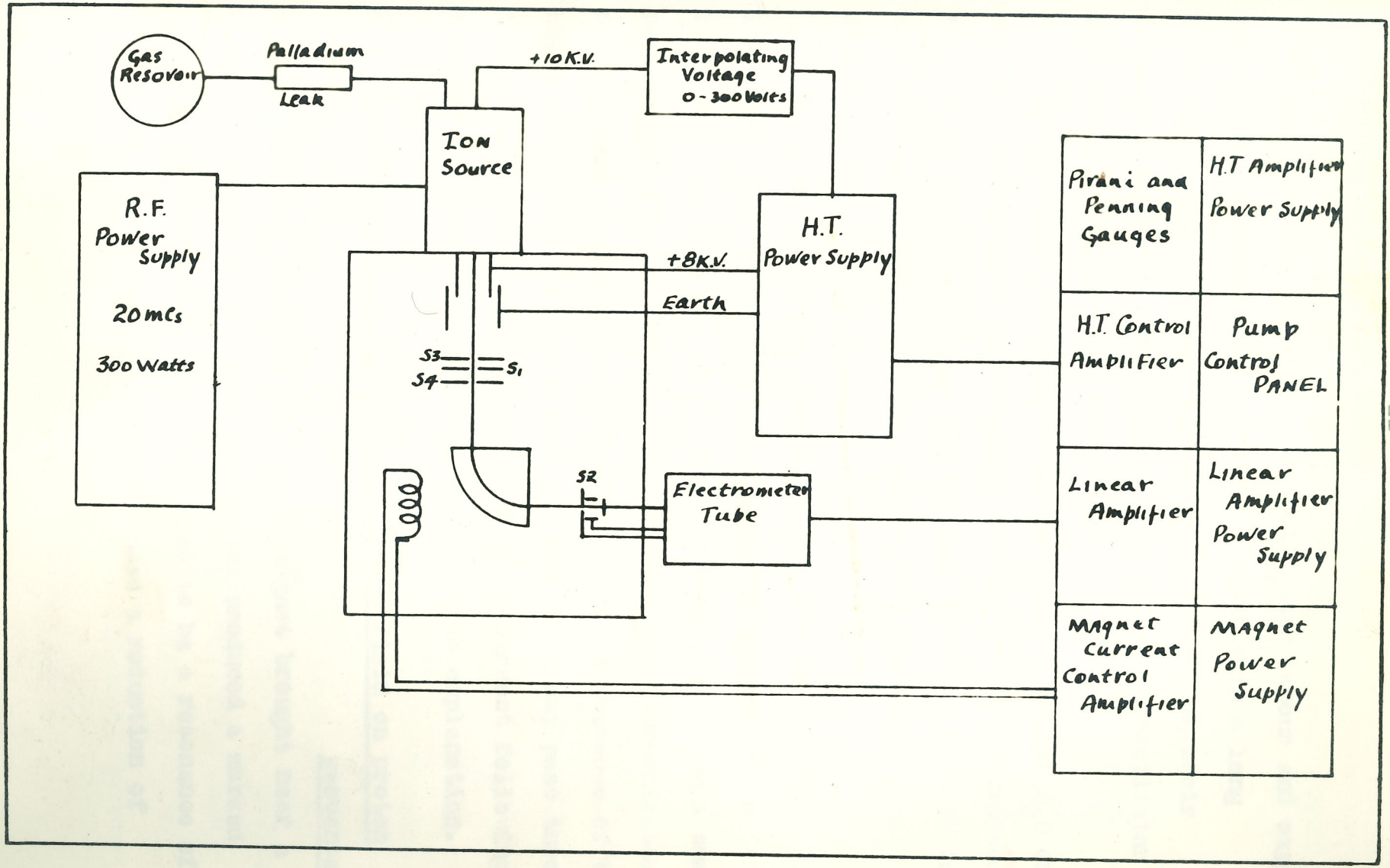


Figure 3. Block diagram of Mass Spectrometer arrangement.

Wood (21) has observed that both water vapour and oxygen increased the number of Balmer lines visible in a long discharge tube. Both these gases were tested for their influence on proton percentage. A 60 megacycle oscillator was used for exciting the discharge.

The presence of a very small quantity of either H_2O or O_2 (not measurable on a pirani gauge reading 0-40 μ) increased the proton percentage from 30% for pure hydrogen to 60%, for the same power input, however, the actual proton current decreased by a factor 6.

Since the ionization potential for the formation of H_2O^+ lies lower than that of H_2^+ or H^+ and the cross section for ionization is greater, it is to be expected that even a small percentage of water vapour will give rise to a concentration of H_2O^+ ions comparable with that of H^+. The presence of these heavy ions decreases the proton current which may pass through the canal. The marked reduction of probe current following the introduction of impurities supports this explanation.

2-7 The influence of a constant magnetic field on proton percentage.

It had been observed that a bar magnet brought near a discharge tube excited at 60 megacycles produced a marked increase in luminosity. This appeared to be a resonance effect of some kind as too large a field caused a reduction of luminosity.

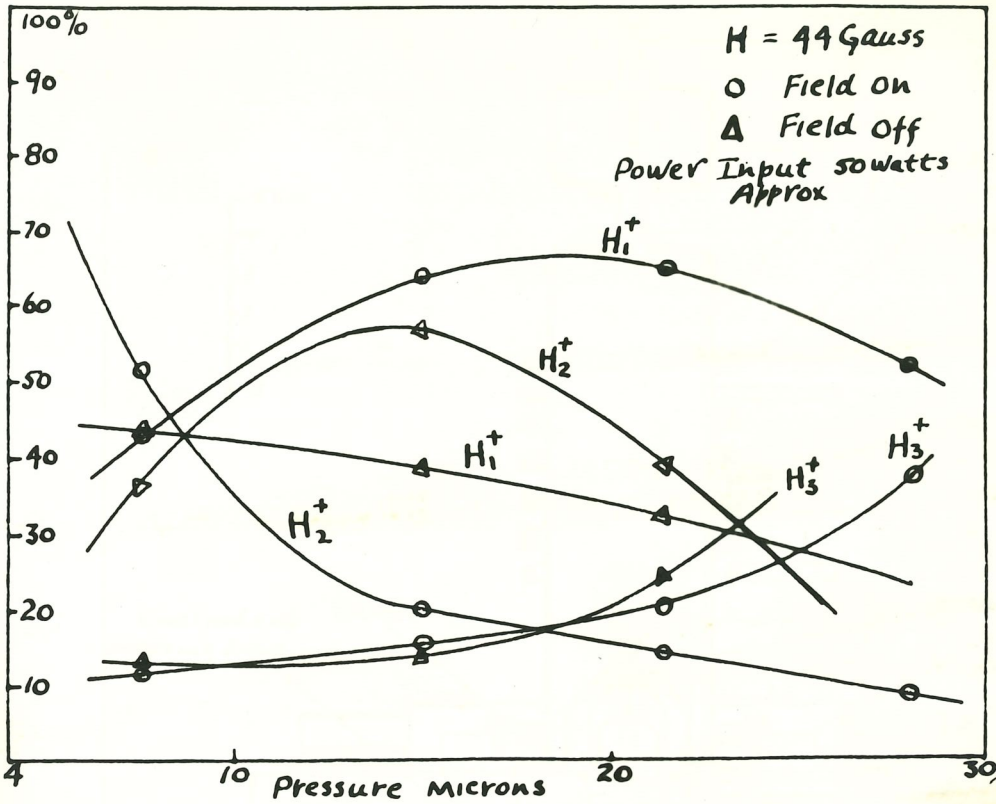
The ion source on the mass spectrograph was surrounded by a Helmholtz coil and proton percentages measured as a function of magnetic field strength. The remarkable variations of proton percentage are shown in Figure 4. The explanation of these results is not known.

In the final ion source, however, no magnetic fields were used as a reduction of the exciting frequency to 20 megacycles in addition to increased power input produced proton percentages up to 90% and an increase of a few per cent did not warrant the use of a magnetic field. Where it is necessary to reduce the exciting power to a minimum the magnetic field can be used to advantage.

2-8 Final ion source design and performance.

The design of the final ion source is shown in Figure 5. The double gasket seal supporting the pyrex envelope permits the probe to be centered in the glass sheath. The level of the probe in the sheath is not critical but the best ratio of beam current to probe current is attained when the probe top is a depth below the sheath top equal to the outside probe diameter. The gas and pressure gauge connections are made through the base of the source. The clearance of 0.5 mm. between the probe and the glass cylinder suffices to admit gas into the envelope.

In order to reduce the D.C. potential across the glass envelope the exciting coil is electrically connected to the anode. More reliable self starting may be obtained, however,



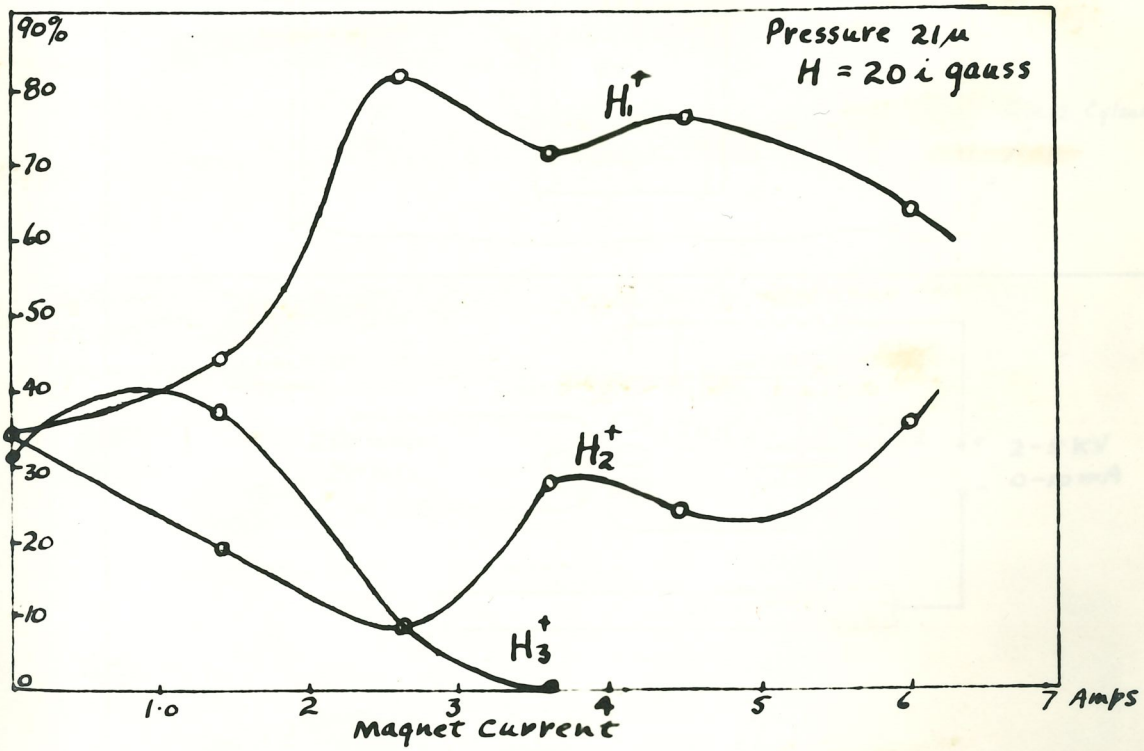


Figure 4. The change of proton percentage as a function of pressure (magnetic field constant) and as a function of magnetic field strength (pressure constant).

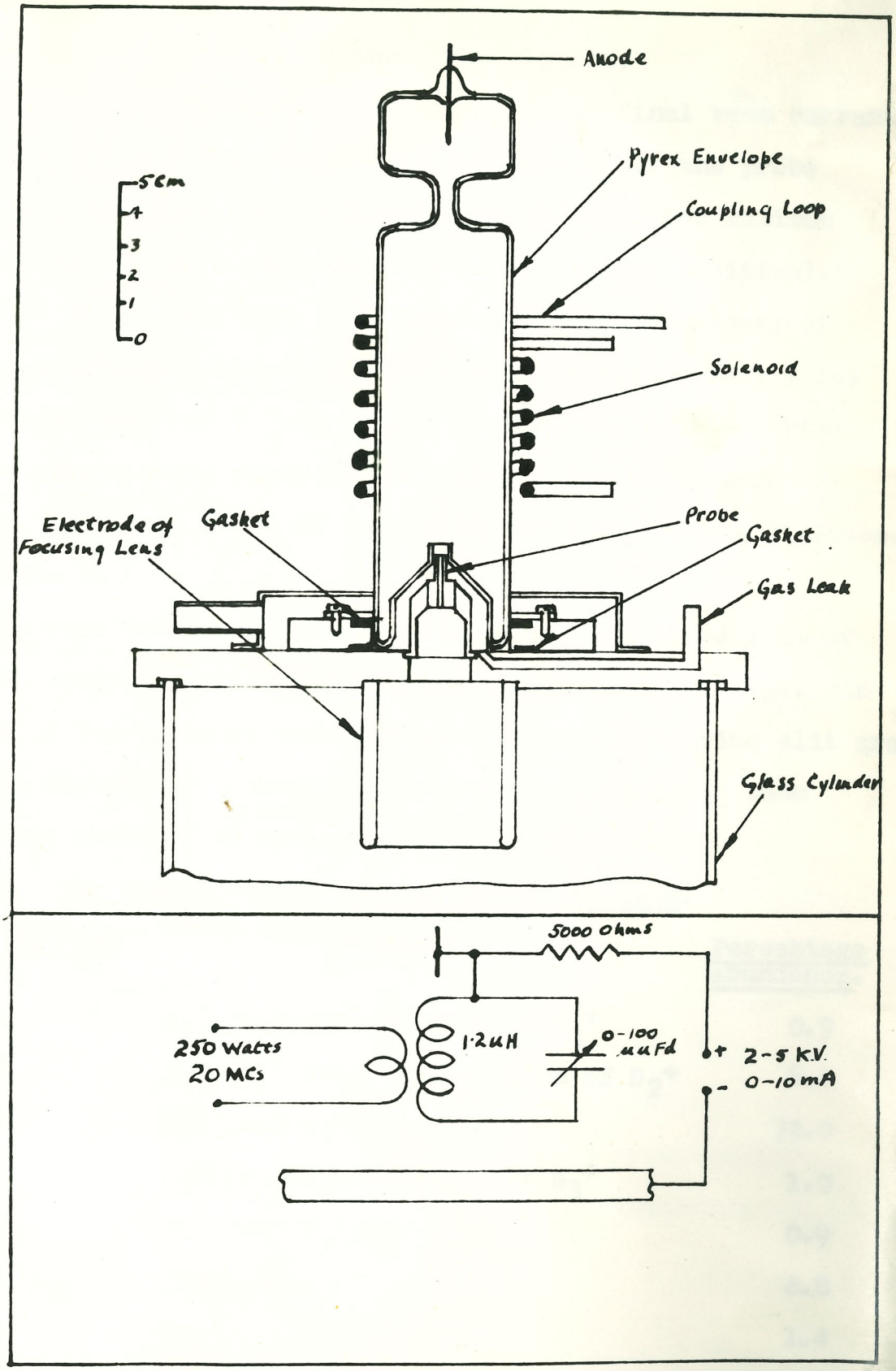


Figure 5. Final ion source design and electrical connections.

if the coil is connected to the probe support.

For a fixed geometrical arrangement the final beam current follows the law $I = \text{constant } V_1^{3/2}$ (where V_1 is the probe potential) provided the ion density is adjusted for maximum beam current (i.e. plasma boundary in stationary position). The value of the constant is a measure of the efficiency of the ion extracting system and has a maximum theoretical value for protons constant = $3.79 \times 10^{-6} R^2/L^2$. The best experimental results give a value approximately 25% of the theoretical maximum. Possible means of increasing this figure are discussed in section 2.

The resolved ion beam was moved across the final slit of the mass spectrograph by varying the accelerating voltage. An example of the contours obtained with a 1 mm. receiving slit are shown in Figure 6. A complete analysis of a deuteron beam containing about 7% of hydrogen is given in Table 2.

Table 2. The mass spectrum of a deuteron ion beam.

Magnet current (ma).	Species.	Percentage abundance.
29	D_1^+ from dissociation of D_3^+	0.9
32	H_1^+; D_1^+ from dissociation of D_2^+	6.0
54	D_1^+ and H_2^+	79.0
60	D_2^+ from dissociation of D_3^+	1.0
62	HD^+ and H_3^+	0.9
80	D_2^+ and H_2D^+	8.8
90	HD_2^+	1.4
99	D_3^+	2.1

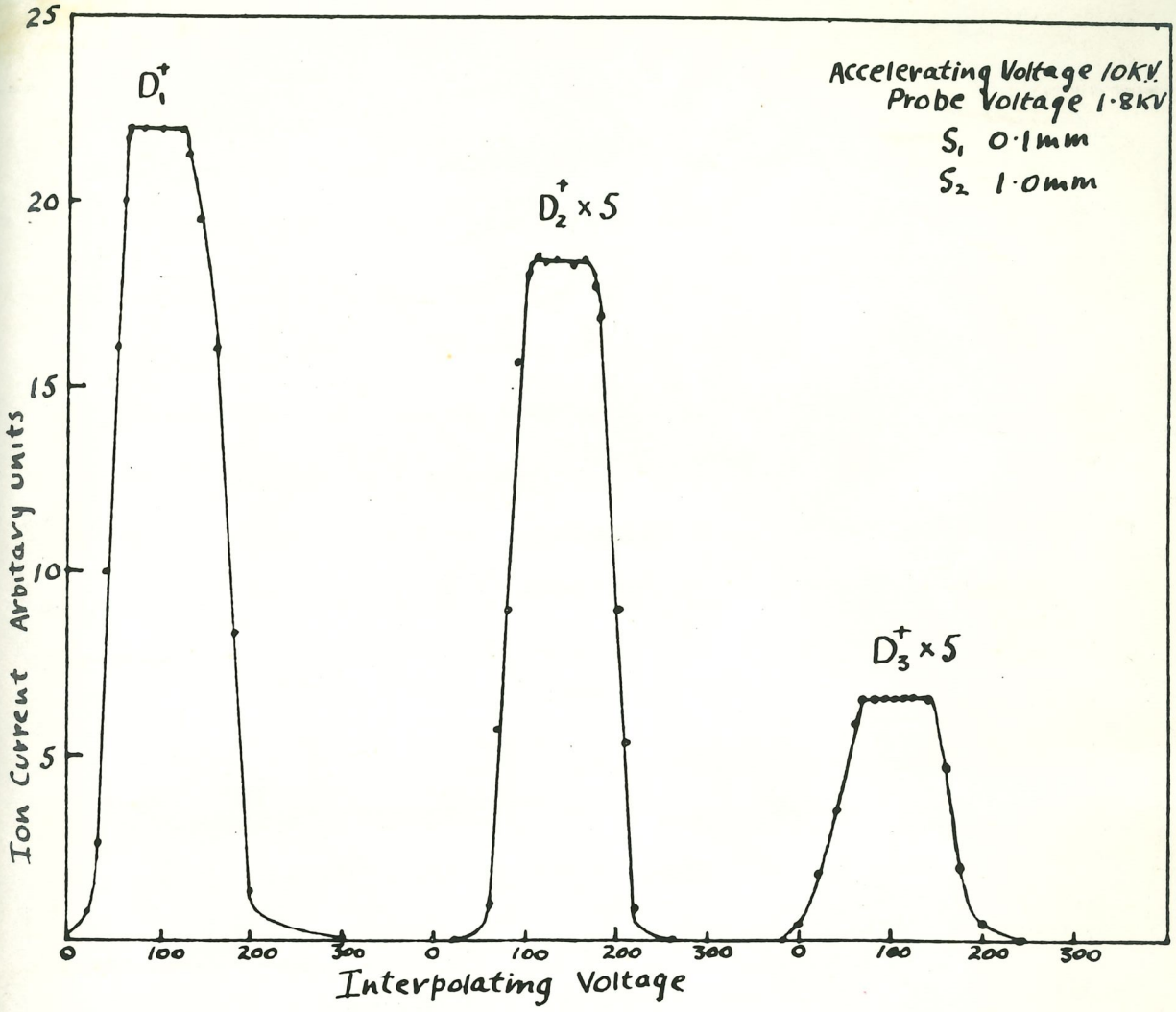


Figure 6. Examples of ion current contours used in computing deuteron percentages.

The half width of the D_1^+ curve was approximately 0.5 ma. The position of the first peak corresponds closely to the energy which a D_1^+ would have if it had been produced by the dissociation of a D_3^+ ion after acceleration according to the reaction :

$$D_1^+ \rightarrow D_1^+ + D_2.$$

The presence of slow D_2^+ ions shows the dissociation

$$D_3^+ \rightarrow D_1 + D_2^+$$

is also possible and has about the same cross section.

A weak line lying close to the D_1^+ line was observed when using a calcium tungstate fluorescent screen in place of the slit S2. The separation between these two lines varied with probe voltage and indicated the production of D_1^+ ions in the canal either by dissociation or direct electron collision. The separation between the lines corresponded to the probe potential. The secondary line was too weak to be detected electrically.

2-9. Variation of proton percentage with R.F. power input.

Various electrical methods were tried in an attempt to measure the total power dissipated in the discharge.

(1) Measurement of voltage at three points spaced $\lambda/8$ apart on the concentric cable (Z_o = 78 ohms) supplying the R.F. power. This method failed because the vacuum tube voltmeter disturbed the voltage distribution on the line. A satisfactory determination could be made if the standing wave ratio was small. This was not the case.

(2) Substitution of a resistance in the resonant circuit associated with the discharge was unsatisfactory because of the difficulty in making a non-inductive resistance which would dissipate up to 300 watts continuously.

(3) Measurement of the "Q" of the resonant circuit was impossibl because of the distortion of the voltage-capacity curve. The

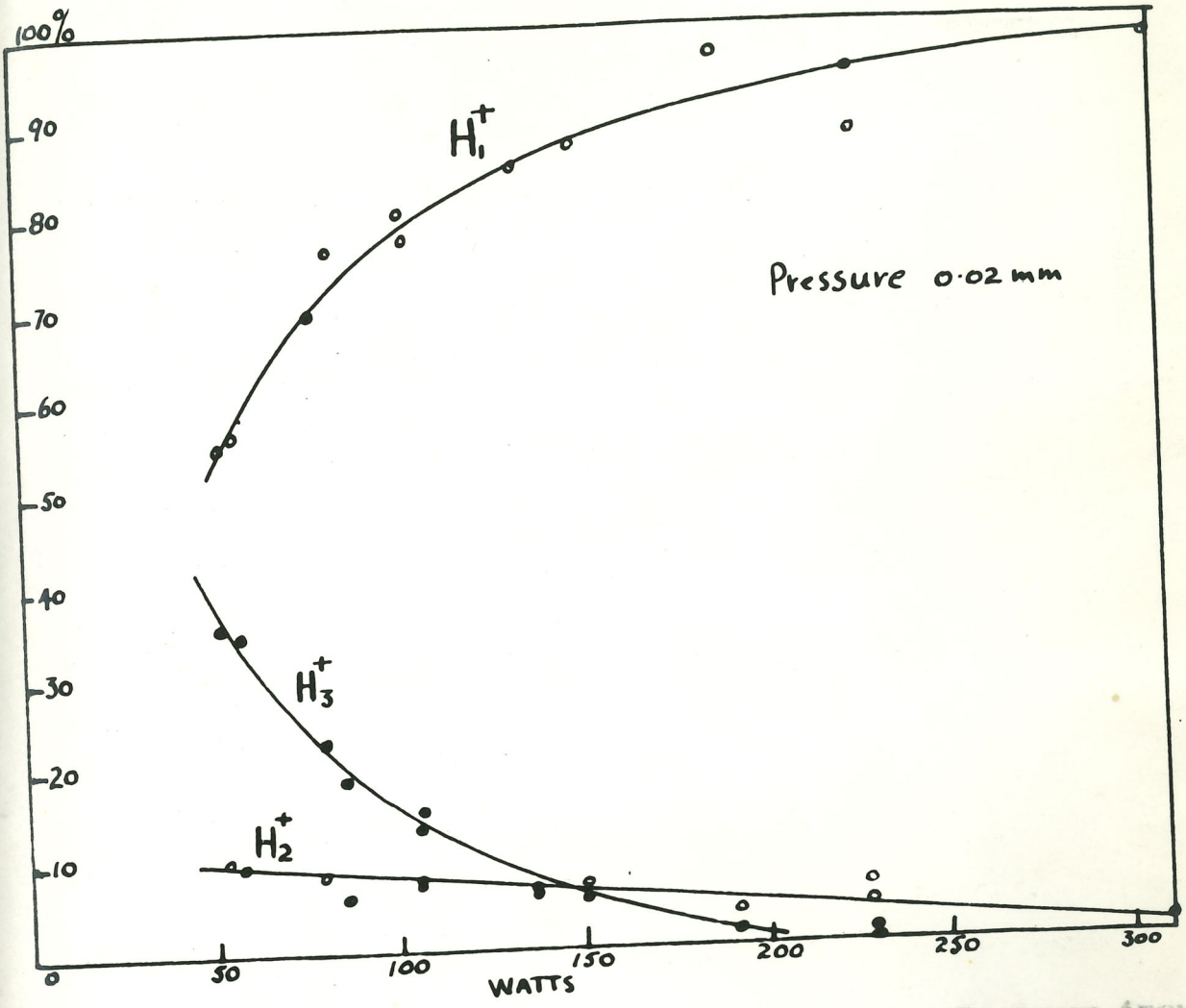


Figure 7. Proton percentage as a function of R.F. power input.

The voltage (1200 volts) across the tuned circuit remained constant within ± 5% over an appreciable range of the tuning capacity.

Provided the ring discharge had struck, the voltage across the coil was independent of power input from 50-300 watts.

The results given in Figure 7 were obtained by measuring

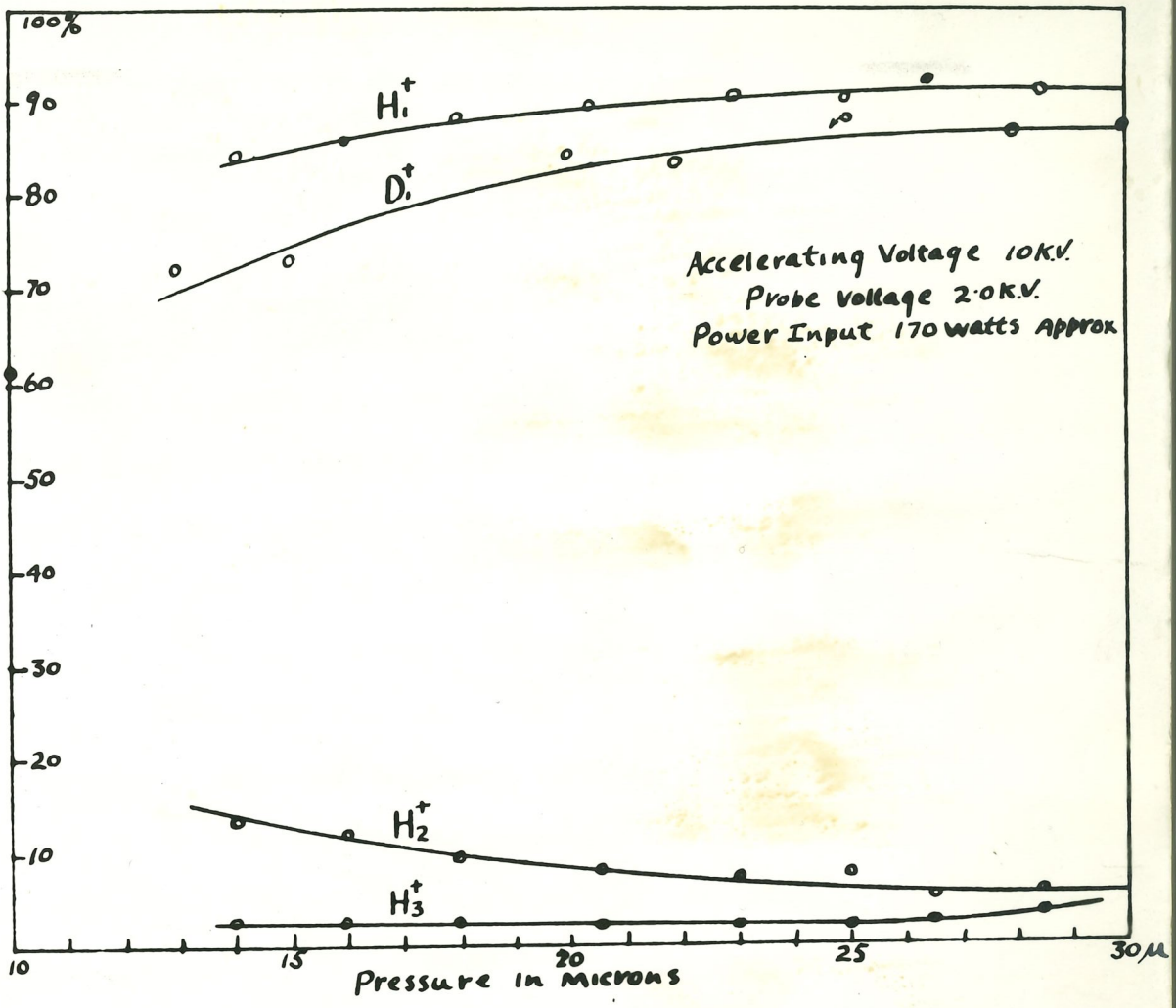


Figure 8. Variation of ion percentage with gas pressure.

the rise in temperature of transformer oil flowing at a known rate through a glass jacket surrounding the ion source envelope. The additional loss in the resonant circuit ($Q = 375$) was 25 watts and independent of power input.

2-10 Variation of proton percentage with gas pressure.

The proton percentage does not change markedly with pressure over the range which could be investigated (13-30μ). The discharge extinguished at the lower pressure. Figure 8

illustrates the results obtained. The reason for the lower atomic ion percentages with deuterium is not clear.

2-11 Energy inhomogeneity of deuteron atomic ions.

The inhomogeneity of the atomic ions was investigated by comparing the theoretical curve for a perfectly homogeneous beam with that obtained experimentally. Figure 9 shows the result. The theoretical computations were made by J. Moffatt taking into account both the focussing aberrations and the finite slit widths. It is concluded that 90% of the atomic ions have an energy inhomogeneity of less than ± 20 volts. The tail on the low energy side is attributed to collisions and energy loss by ions in the high vacuum side of the apparatus. The tail increased in amplitude and length with poorer vacuum conditions.

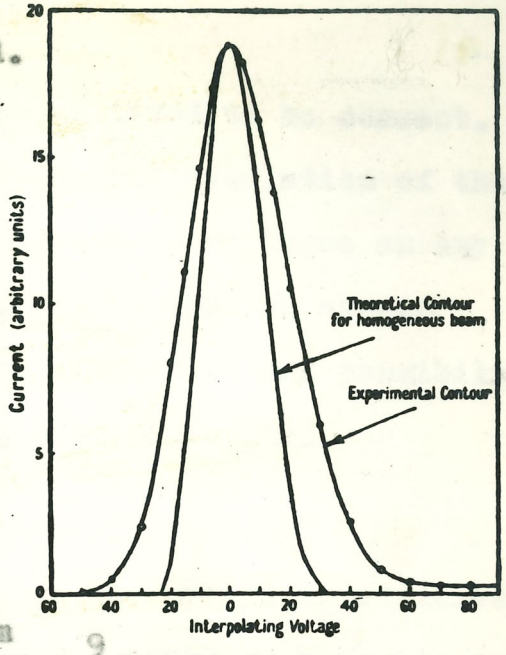


Figure 9 Comparison of the theoretical contour for a homogeneous beam with the D_1^+ ion contour. $V_p = 3$ kv., $V_a = 10$ kv., $\rho = 20\,\mu$; $s_1 = 0{\cdot}1$ mm.; $s_2 = 0{\cdot}1$ mm.

90% of the ions which finally pass through the canal are formed in a region over which the potential varies by an amount given by $eV = 2.3\ kT_1$ where T_1 is the electron temperature. Assuming molecular hydrogen gas this potential difference amounts to 31.5 volts (section 1-3). Although the electron temperature is expected to be lower in atomic hydrogen this

explanation of the inhomogeneity is believed to be correct.

Care was taken to reduce any possible modulation of the ion energy by R.F. voltages. The measured R.F. voltages on any electrode was less than 2 volts R.M.S. A Faraday screen surrounding the ion source envelope eliminated any possibility of direct R.F. modulation of the plasma potential.

2-12 Conclusion.

The electrodeless ring discharge has proved an efficient method of coupling quite high radio frequency powers into an ionized gas with the consequent production of high ion density at low pressures. Ion beam currents have never been limited by insufficient ion density. Further progress could be expected from a closer study of the focussing of the ions into the canal. Only 25% of the maximum theoretical ion beam currents have yet been achieved chiefly due to the difficulty in bringing the ions to a focus at the canal centre and collecting them from the requisite solid angle.

Experimental determination of the D-D branching ratio.

3-1 Introduction.

Previous investigations of the D-D reaction have established the following reactions :

$$\left.\begin{aligned} {}_1D^2 + {}_1D^2 &\rightarrow {}_1H^1 + {}_2H^3 + 3.98 \text{ MV} \\ &\rightarrow {}_1He^3 + {}_1n^0 + 3.18 \text{ MV} \end{aligned}\right\} \text{ Disintegration}$$

$$\rightarrow {}_1D^2 + {}_1D^2 \quad \text{scattering.}$$

The reaction energies are those given by Bonner and Brubaker (48) and Oliphant, Kempton and Rutherford (47).

No direct comparison of the ratio of the probability of the two disintegration reactions has appeared in the literature* although qualitative cloud chamber observations (50) have indicated approximately equal probabilities ($He^3/H^1 = 0.8 \pm 1$). Measurements have been made by J.H. Coon et al. (51) of the disintegration cross section for the two reactions by comparing the neutron yield with a standard radium-beryllium source and direct counting of the proton yield. A 15% accuracy is claimed in both experiments but two separate attempts to calibrate the standard neutron source gave results differing by a factor two.

A direct comparison by counter technique of the number of H^1 and He^3 nuclei is difficult because of the short range of the He^3 nuclei (4.3 mm. (52)). Because of the importance of establishing a standard source of fast monochromatic neutrons

* See Appendix II.

as well as theoretical interest in the branching ratio an attempt is described here to determine this ratio by a direct measurement of the number of H^1, H^3 and He^3 nuclei in proportional counters.

3-2 Preparation of the counter windows.

The success of the proportional counter method depended on the preparation of a window sufficiently thin to have a stopping power for alpha particles small compared to 4.3 mm. of air and capable of withstanding a pressure difference of 10 cm. of mercury. Collodion films prepared by evaporation on a water surface could not be made strong enough to withstand the pressure difference when covering the 3 mm. diameter hole admitting particles to the counter. Silica films prepared in the following manner proved, however, to be very satisfactory. A 5 mm. outside diameter clear silica tube is put in an oxygen-gas flame adjusted for maximum heating. The tube is blown into at the instant of withdrawal from the flame and results in a bubble, sections of which show interference colours in white light. These pieces were collected and used for counter windows.

The windows were mounted on a support of insulating material in the following way. A thin layer of soft wax was first run round the aperture to be covered, then holding the film in a pair of forceps with the convex side towards the support, the wax was momentarily melted with a small gas flame and the film gently blown into place. Generally it attached itself at two or three points but by holding a soldering iron

at a distance of 2 or 3 mm. the wax was melted and surface tension draws the window into place. Of some ten windows prepared in this fashion, none have leaked.

A window showing bright interference colours covering a 3 mm. diameter hole has been observed to stand a pressure difference of 40 cm. of mercury. In general the more uniformly the film can be attached the higher the pressure it will withstand. Similar windows made of soda or pyrex glass, though initially as strong as silica, usually break after about half an hour. Silica windows do not appear to deteriorate after a week of use under bombardment. Films showing interference colours in white light will just transmit 82 K.V. deuterons and have an estimated stopping power equivalent to 1.4 mm. of air.

3-3 Relative pulse amplitude due to H^1, H^3 and He^3 nuclei.

The energies of the three charged particles emitted in the D-D disintegration are :

H^1	3.00 MeV.
H^3	0.98 MeV.
He^3	0.80 MeV.

The theory of the energy loss by inelastic collisions of charged particles has been given by Bethe (58) on the basis of Born's approximate treatment of collision processes. Bethe's formula is derived on the assumption that the velocity of the incident particle is large compared to the electron velocity in the atom.

Under these conditions the energy loss per cm. path is :

$$- dE/dx = 4 e^4 z^2/mv^2 NB$$

$$\text{With } B = Z \log_e(2 mv^2/I)$$

in which v is the velocity and eZ the charge of the incident particle, N the number of atoms/cm^3 of the material, Z the nuclear charge, and I the average excitation potential of the atom.

The region of validity of the above formula is theoretically restricted to particles of high energy, e.g. for oxygen the ionization potential of the K shell is about 540 volts and the above equation is valid for alpha particles above 4 M.V. It has been shown, however, (59), that the general principles of Born's approximations can be applied to the collision of heavy particles with atoms down to velocities much lower than that of the atomic electron.

Since the energy of the He^3 nuclei is relatively low the capture and loss of electrons will have an important influence on the energy loss. No adequate theory is yet available for dealing with this case. It is clear, however, that the energy loss/cm. will be less than calculated from Bethe's formula, since the time average of the particle's charge will be less than that at high energy where charge exchange is negligible.

The relative energy loss/cm. for the three nuclei based on Bethe's formula is H^1 : H^3 : He^3 : : 1 : 3 : 15. The relative

ionization based on the results obtained with the pulse amplitude selector is 1 : 3 : 9. The difference is attributed to charge exchange of the He^3 nuclei. Alpha particles of energy 0.5 MeV. have a measured mean free path for electron capture in air of 1 mm. at 1 mm. pressure (53). The mean free path for the reverse reaction is of the same magnitude; so that an alpha particle of this energy spends roughly half of its time as a singly charged particle and the rate of loss of energy must be reduced below that calculated from Bethe's formula.

3-4 Preliminary experiments.

A water cooled copper block inclined at 45° to the 100 K.V., 200 A deuteron beam served as a target. Deuterium driven into the copper supplies an adequate yield of disintegration particles. The product nuclei emerging at 90° to the incident beam are collimated to a 3° half angle and pass into a small proportional counter filled in situ with a 90% argon 10% alcohol mixture at 10 cm. pressure. The counter was connected to a linear amplifier of conventional design built for the purpose.

Based on information given by Livingston and Bethe (52) and including the loss of energy by the three nuclei in escaping from the target and passing through the window, the ratio of pulse amplitude should be He^3 : H^3 : H^1 : : 15 : 3 : 1. Pulses of this approximate amplitude ratio were observed on an oscillograph and it was concluded that all three nuclei were being counted. The degree of separation of the pulse groups was examined on a twin channel pulse amplitude selector for

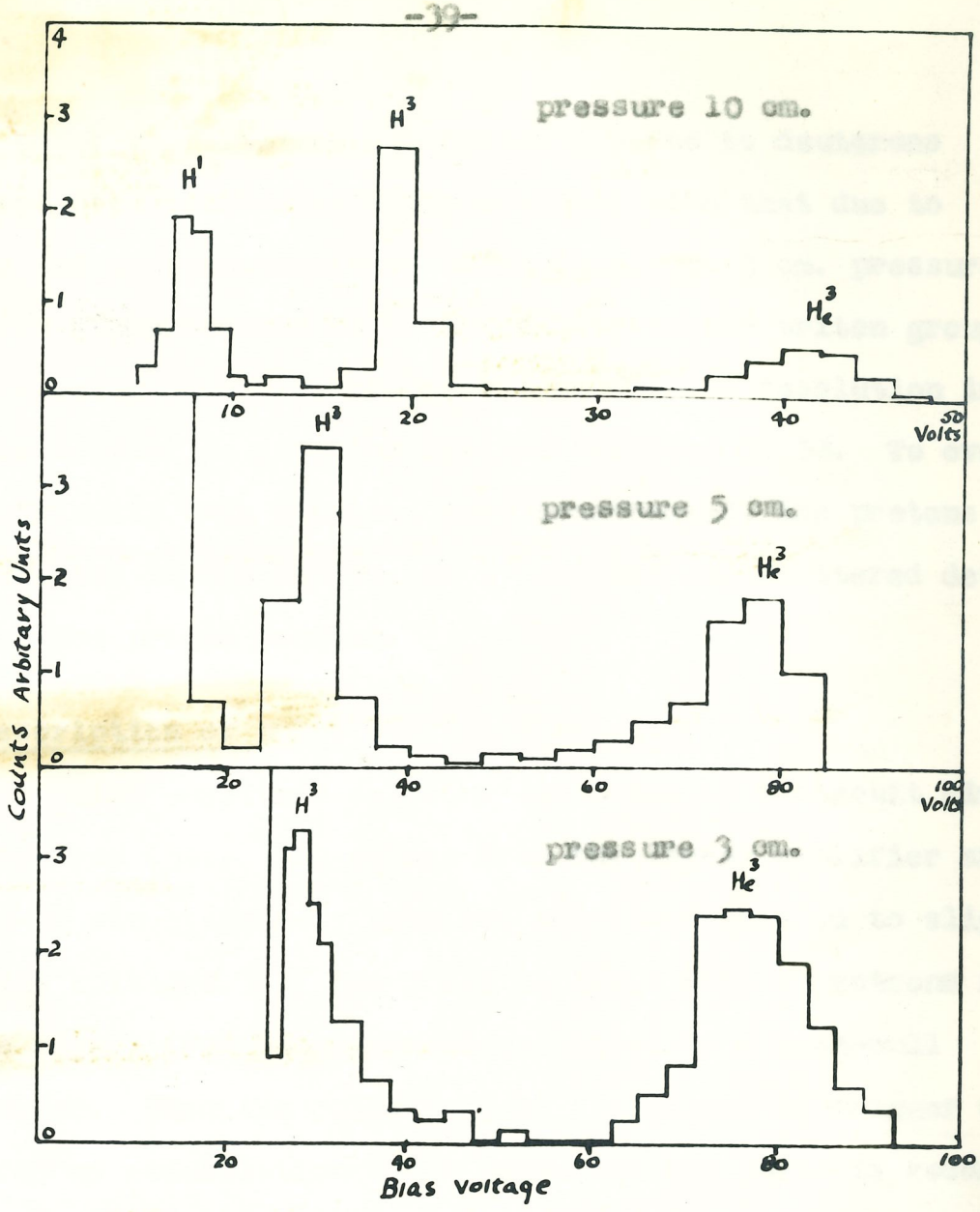


Figure 10. The resolution of the three particle groups in a single proportional counter. Filling 90% argon 10% alcohol.

different counter pressures. The results are shown in Figure 10 for three different pressures. At 10 cm. pressure all three groups could be readily identified but the resolution of the He^3 and H^3 peaks was insufficient for quantitative measurements. At 5 cm. pressure good separation of the He^3

and H^3 peaks was obtained but ionization due to deuterons scattered from the target was comparable with that due to protons and measurements were impossible. At 3 cm. pressure scattered deuterons had begun to obliterate the triton group. It was clearly impossible to obtain sufficient resolution in a single counter to give the desired accuracy of 5%. To overcome this difficulty twin counters were constructed, the protons being counted in the second and H^3 and He^3 and scattered deuteron entering the proton counter. the first. An aluminium window 0·0005" thick prevented He^3, H^3

3-5 Description of pulse amplitude selector.

The pulse amplitude selector was based on a circuit given by A. Roberts (54). The pulses from the linear amplifier are introduced simultaneously into two thyratrons biased to slightly different voltages. If the pulse is large both thyratrons fire and the signal from both thyratrons cancel in a push-pull transformer. When the pulse is just sufficient to trigger one thyratron no cancellation takes place and the pulse is recorded in a scaler. Pulse of amplitude insufficient to trigger either thyratrons are not recorded. The circuit given by Roberts was found unsatisfactory due to "ringing" in the push-pull transformer The ratio of cancelled pulse to uncancelled pulse could not be made better than 3 to 1. A triode valve was substituted for the push-pull transformer and arranged so that where both thyratrons were fired negative pulses from each were applied simultaneously to the grid and cathode of the triode and no signal pulse

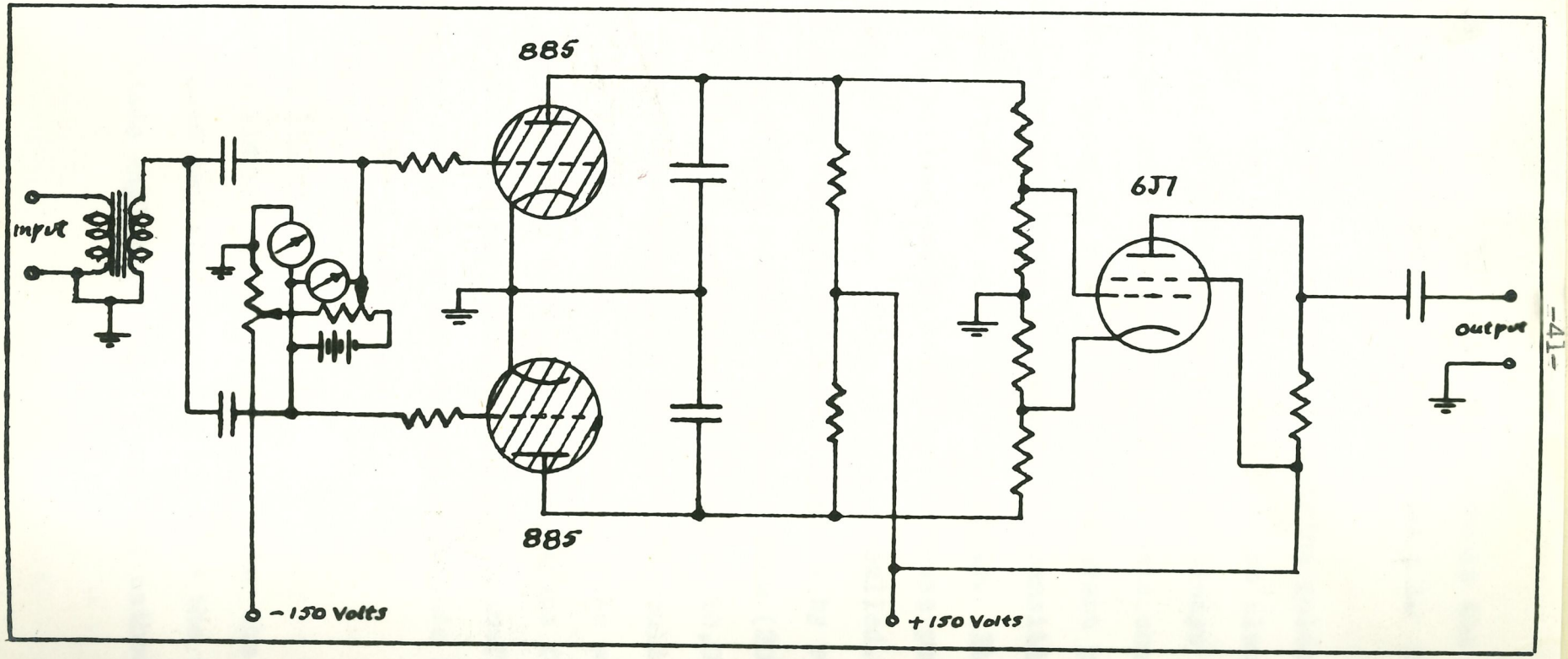


Figure 11. Pulse cancelling circuit of pulse amplitude selector.

appeared in the plate circuit. With this circuit the amplitude ratio of cancelled to uncancelled pulse was 50 : 1. The diagram of this circuit is shown in Figure 11.

Due to the finite rise time of the incoming pulse and the difference of bias on the thyratrons one thyratron always fires before the other and an initial short pulse is always transmitted. However, by a slight unbalance in the circuit this short cancellation pulse could be made to have a different polarity to the uncancelled pulse and since the scaler was sensitive to pulses of only one sign this caused no difficulty. It was possible indeed to monitor on an oscillograph those pulses which were cancelled and those which were uncancelled. The resolving power of the circuit was made a maximum by reducing the plate potential of the thyratrons to a minimum (20 volts). The thyratron circuit self oscillated at close to 10,000 cycles per second and it was concluded that the circuit would record pulses separated by 10^{-4} seconds. The counting rate was generally kept below 300 per minute so that the cross sections for the finite resolving time were negligible. A pulse transformer on the input raised the maximum output voltage amplitude from the linear amplifier from 50 to 100 volts.

3-6 Description of linear amplifiers.

A conventional linear amplifier was built for the initial experiments. The head amplifier mounted close to the counter consisted of a pentode amplifier first stage and cathode follower

matching into the 80 ohm concentric cable leading to the main amplifier chassis. The amplifier valves employed had a mutual conductance of 12 mA/volt. The amplifier had a maximum gain of 4000 and a band pass from 1000 c/s to 1 megacycle. The resistance capacity coupling circuit between the pentode and cathode follower in the head amplifier had a time constant of 10^{-4} seconds. The remainder of the resistance capacity circuit had a time constant of more than 10^{-2} seconds. The short time constant coupling circuit serves two purposes, (a) to attenuate 50 cycle pick-up in the first amplifier stage, (b) to eliminate low frequencies components in the counter pulse and thus the back kick due to long time recovery in the other coupling circuits. The amplifier proved very stable. In the experiments with the twin counters an additional linear amplifier and discriminator of commercial design were employed.

3-7 Description of twin counter arrangement.

A drawing of the final target and twin counter arrangement is shown in Figure 12. The disintegration products from the target passed through two collimating holes in a cylinder of polytetrafluorethylene. The silica window was waxed into the counter end of the collimator. The dimensions of the counter were such that the He^3 nuclei could just cross the counter when filled with 90% argon 10% alcohol mixture at 6 cm. pressure. Protons entered the second counter through a 6 mm. hole and a slide mounting the aluminium foil could be placed between the

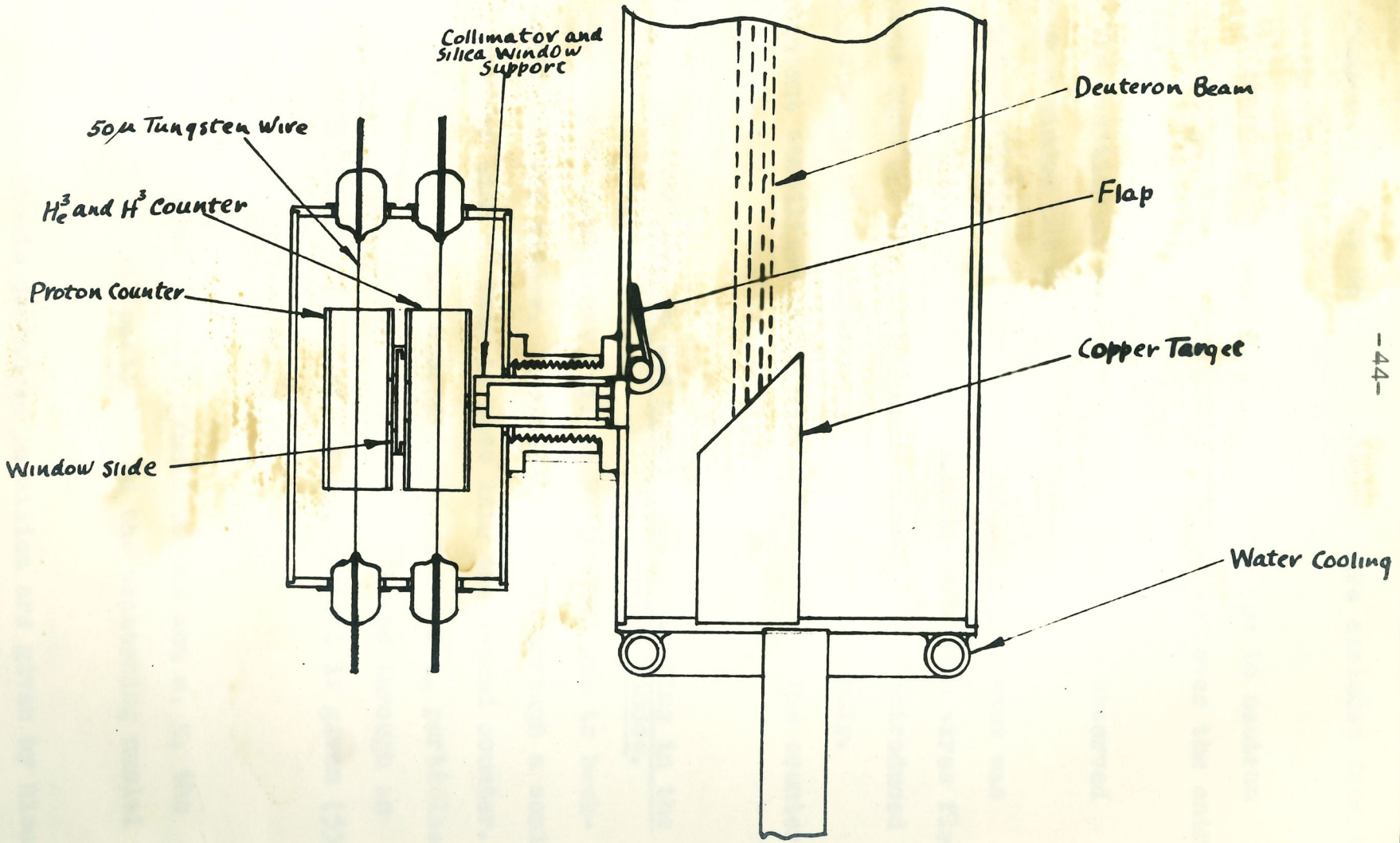


Figure 12. Target and twin counter arrangement.

two counters so that He^3 and H^3 nuclei were excluded from the proton counter.

In order to determine the background due to neutron recoils and gamma rays a flap could be placed over the entrance hole of the collimator.

The position of the beam on the target was observed through a window not shown in the diagram.

Before filling the counters the whole apparatus was evacuated on the accelerator and the 50 tungsten wires flashed at about 2000°C. The argon alcohol mixture was introduced from a storage flask attached to the target assembly. Independent stabilized power supplies furnished the counter voltages.

3-8 Loss of particles by the Rutherford scattering in the silica window.

He^3 and H^3 nuclei may fail to be counted due to back-scattering in the window. Protons scattered through a semi angle greater than 3° fail to pass into the second counter.

If the initial beam consists of a flux of I_0 particles per second of energy T, the number I scattered through an angle greater than in a foil of thickness t is given (55) by:

$$I/I_0 = Nt(Ee/T)^2 \cot^2 \phi/2$$

where N is the number of nuclei/unit volume and e, E, the charges of the incident particle and the scattering nuclei respectively.

The inter-atomic distances in silica are given by Rice (56)

as 1.58 Å, and N becomes 4.0×10^{23} atoms/cm^3. The thickness of the silica window was taken to be 5×10^{-5} cm. The number of back-scattered He^3 and H^3 nuclei turns out to be completely negligible and only 0.2% of the protons penetrating the window are scattered beyond a 3° semi angle and not counted.

3-9 Background due to neutron recoil nuclei.

The solid angle subtended by the active volume of the counters at the target is approximately 50 times that of the particles passing through the collimator. The collision cross sections of 2.5 MeV. neutrons with H, C and O lie in the range 1 - 2.5 barns (57). Assuming argon to have a cross section of similar magnitude the total cross section for neutron collision is approximately 1.2×10^{-5} cm^2/cm^3 for a counter at 6 cm. pressure 90% argon 10% alcohol.

Taking into account the smaller area of the beam subtended by the collimator and assuming a branching ratio of unity the ratio of the number of pulses due to neutrons and due to H^1, He^3 or H^3 is 6×10^{-3}. It is concluded that neutron recoil nuclei can make an appreciable contribution to the total background count.

3-10 Background due to gamma rays.

It is difficult to understand how gamma rays coming from the target, with a flux equivalent to the neutron flux, could produce any appreciable background count. The ionization produced by Compton electrons crossing a counter is negligible compared to the protons. When a weak radium gamma ray source

(3 millicuries) was brought near the counters pulses equal and greater in magnitude to those of the protons was observed. It is believed, however, that these pulses were again due to neutron recoil nuclei since neutrons can be produced by most natural radioactive substances by the (α, n) reactions.

Rough absorption measurements indicated gamma rays of about 1.6 MeV. coming from the target. The most likely source of this radiation is the (n, γ) reaction in copper. However, the possibility of an excited state of the He^3 or H^3 nuclei cannot be completely excluded. Small peaks lying half way between the main He^3 peak and the H^3 peak were indeed observed in all the pulse spectrum measurements. If this is due to slow He^3 nuclei their energy would be roughly 0.4 MeV. and would be associated with a gamma ray of 1.6 MeV. Because of the small height of these peaks (less than 3% of the main peak) the evidence is most inconclusive. This aspect of the work is being pursued at the present time.

3-11 Method of measurement.

Figure 13 shows a block diagram of the counting arrangement. Immediately after filling the counters the pulse height continued to increase for a period of about thirty minutes and thereafter remained constant. This behaviour is attributed to adsorption of alcohol on the walls of the counter with a consequent increase in the counter amplification. When the pulse heights had ceased to change the voltage on the proton

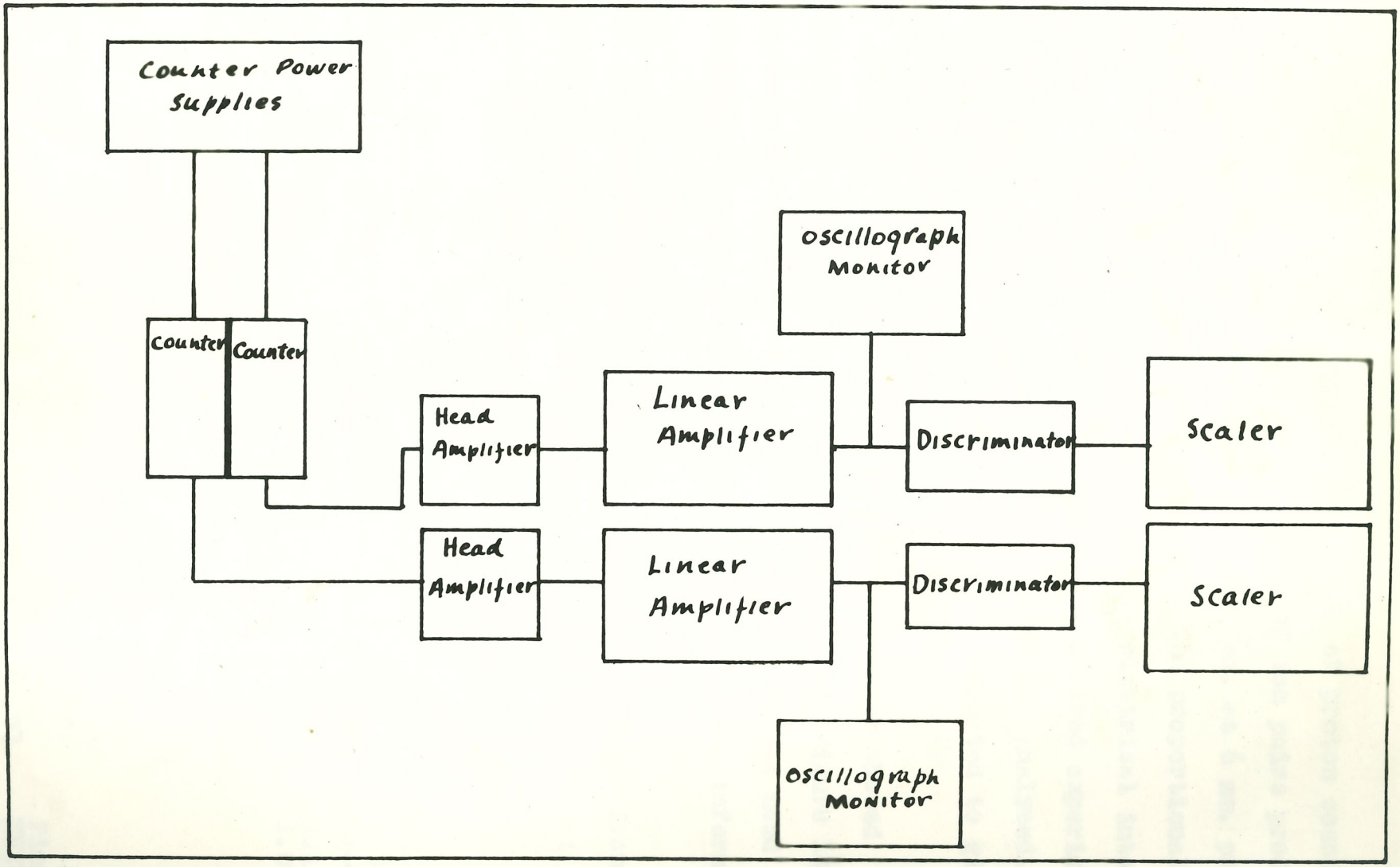


Figure 13. Block diagram of apparatus used in counting.

counter was reduced to give the best ratio of proton counts to background. Because of the small number of ion pairs produced by the protons (approximately 60 ion pairs/cm. at 6 mm. pressure) the counter had to be operated well up in the proportional region to avoid microphonics and excessive electrical interference. A proton plateau flat within the desired experimental accuracy of 5% was found when the bias curve was analysed.

The intensity of the deuteron beam was adjusted to give about 300 counts per minute.

The bias curves taken with the first counter showed plateaux corresponding to H^1, H^3 and He^3 nuclei (Figure 14). To determine the He^3/H^3 ratio the proton counter was used as a monitor so that a single bias curve contains also information on the He^3/H^1 ratio.

Many runs were spoilt by electrical interference from an unknown source which defied elimination. The results obtained are shown in Table 3 below :

Table 3.

82 ± 5 kV.		111 ± 5 kV.		139 ± 10 kV.
He^3/H^1	He^3/H^3	He^3/H^1	He^3/H^3	He^3/H^1
0.80 ± .02	0.88 ± .06	0.90 ± .04	0.87 ± .07	1.11 ± .05
0.87 ± .03	0.86 ± .05	0.89 ± .02	0.85 ± .03	1.09 ± .05
0.87 ± .03	0.84 ± .05	0.89 ± .02	1.03 ± .03	
0.89 ± .03	0.84 ± .04	0.91 ± .03	0.98 ± .06	
0.84 ± .03	0.82 ± .09	0.93 ± .02	1.07 ± .02	
Mean		Mean		
0.85 ± .03		0.93 ± .06		
correction for plateau slope + 0.01		correction for plateau slope + 0.01		
Final Result 0.86 ± .04		Final Result 0.94 ± .07		Final Result 1.11 ± .08

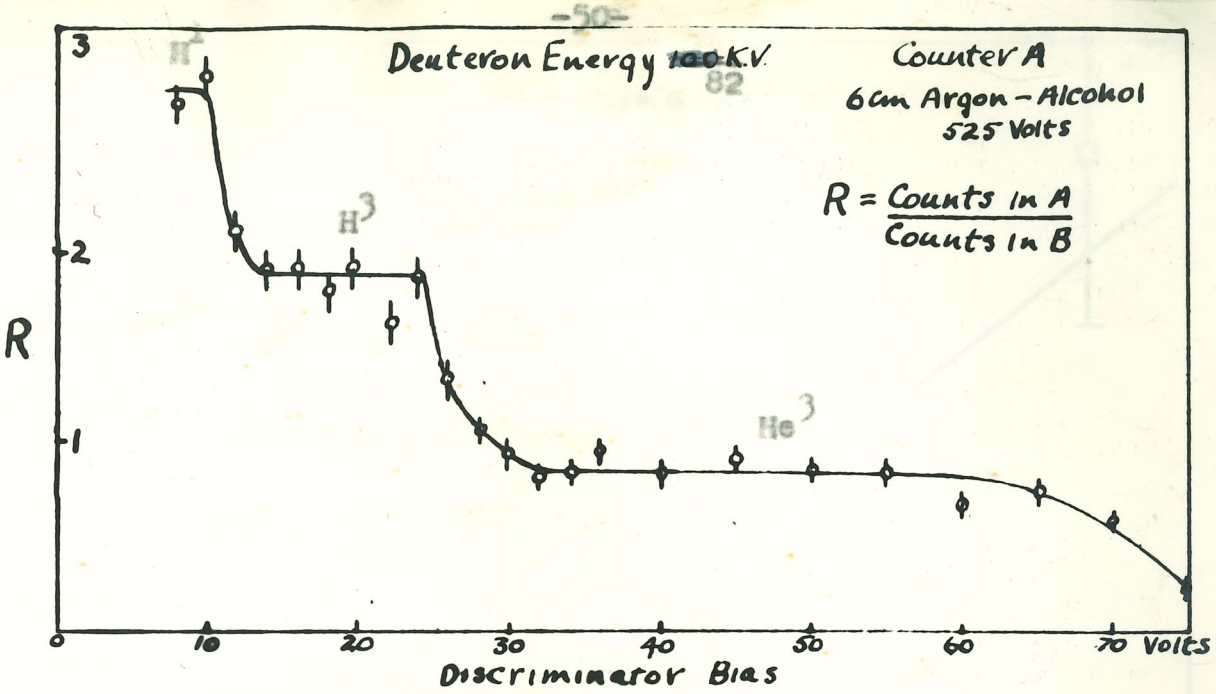


Figure 14. Bias curve showing three plateaux corresponding to He^3, H^3 and H^1 groups.

3-12 Discussion of results.

The excellent agreement between the ratio determined independently from the H^1 counts and the H^3 counts provide evidence for small if not negligible systematic errors in counting protons and tritons. However statistical counting errors for He^3 do not permit a determination of the plateau slope. This has been estimated from the results obtained with the pulse amplitude selector. At a counter pressure of 5 cm. the separation between the He^3 peak and H^3 peak was not complete. This incomplete resolution is attributed to straggling of the He^3 nuclei stopped in the gas. At 3 cm. pressure resolution was complete. This fact provides evidence that the He^3 nuclei entering the counter did not possess energies extending down to zero. The 1% correction for the

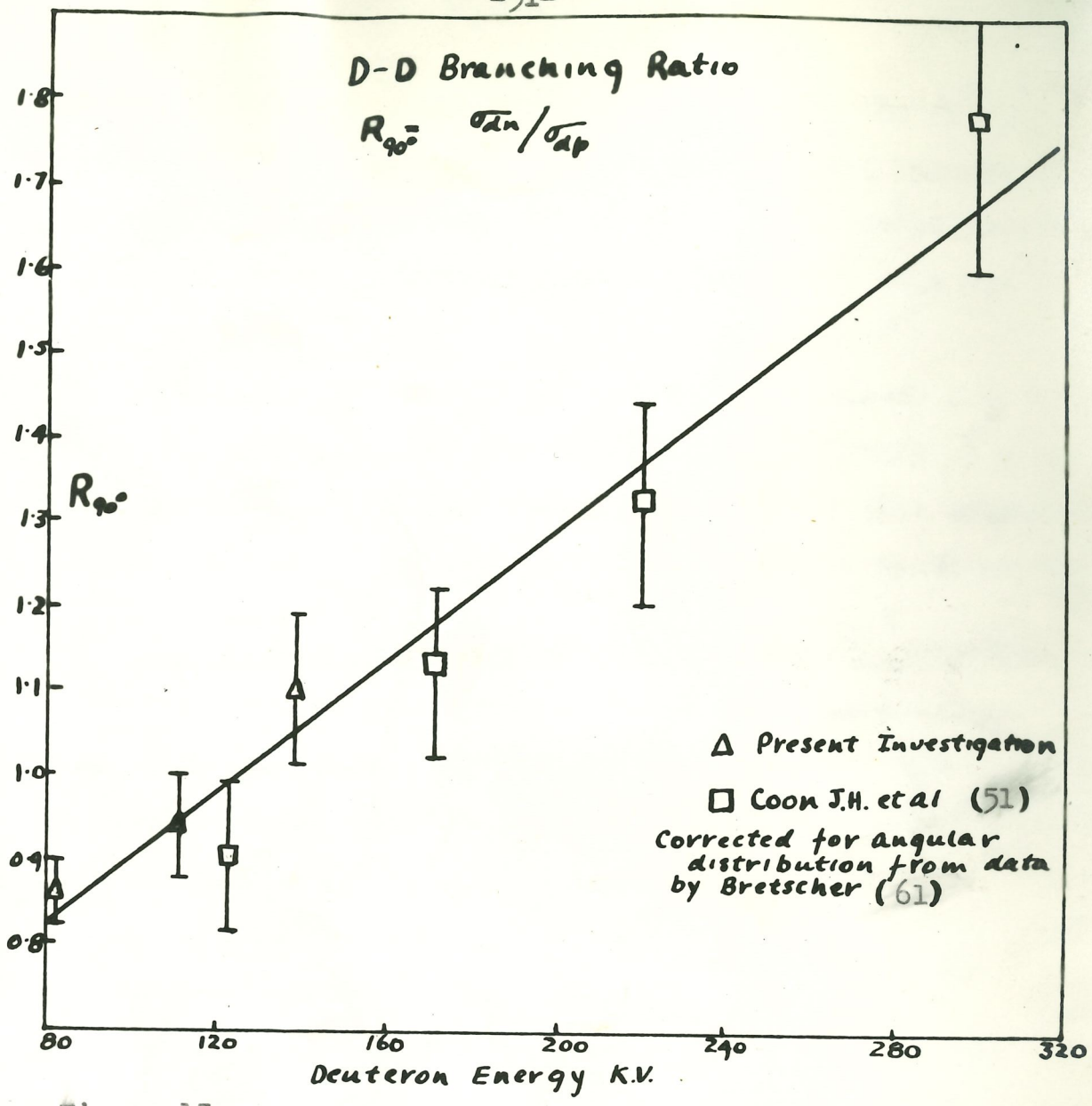


Figure 15.

plateau slope has been estimated on the basis that the ratio of maximum to minimum ionization of He^3 nuclei was approximately 2 to 1 in the counter used. It is likely that varying background counts and electrical interference caused larger errors. At bombarding energies above 82 kV. scattered deuterons entering the first counter reduced the length of the H^3

plateau introducing greater errors in computing the He^3/H^3 ratio. This is reflected in the poorer agreement between the independently measured ratios. At 139 K.V. scattered deuterons had masked the H^3 plateau to such an extent that only the He^3/H^1 ratio could be used.

The results obtained are compared with those of J.H. Coon et al (31) in Figure 15. The agreement is certainly as good as can be expected in view of the unknown errors in the determination of the flux of neutrons from their standard Ra-Be source.

3-13 The absolute cross section for the $D(D,n)He^3$ reaction.

Based on a recent determination of the absolute cross section of the $D(D,p)H^3$ by Bretscher, French and Seidl (61) it is possible to give a more accurate value for the $D(D,n)He^3$ reaction than hitherto. Since the angular distribution of the emitted neutrons is not known for bombarding energies below 0.5 MeV (62) the cross section is computed for neutrons emitted at 90° to the incident beam. (Because of the low energies, less than 139 K.V. the emission angles in the laboratory system never differ from angles in the centre of gravity system by more than 3°).

The cross section σ_{dn} at 90° to the incident beam is given by :

$$\sigma_{dn} = \sigma_{125} / 1 + A \cos^2$$

where A is the assymmetry coefficient and $_{125}$ the cross section for the integrated yield. The values adopted are :

	82 K.V.	111 K.V.	139 K.V.
A	0.37	0.43	0.50
$_{90}$ (D,p)	1.69×10^{-26}	2.28×10^{-26}	3.08×10^{-26}
Branching ratio	0.86	0.94	1.11
$_{90}$ (D,n)	1.45×10^{-26}	2.14×10^{-26}	3.42×10^{-26}

These results are compared with those of J.H. Coon et al in Figure 16.

3-14 Discussion on theory.

Up to the present time no attempt appears to have been made to calculate the relative probability of the two possible D-D reactions. Attempts have been made to derive an absolute value for the reaction cross section from the magnitude of the nuclear forces (63,64,65,66,67). These authors contented themselves with estimates of the order of magnitude of the cross section and do not discuss a nuclear model which might be of value in discussing the branching ratio.

Compound Nucleus Model.

In the interaction of light particles (neutrons, protons, deuterons, etc.) with heavy nuclei the concept of a compound nucleus has provided an explanation of both qualitative and quantitative features.

The incident nuclei on collision, is caught, and distributes its energy amongst the particles comprising the heavy nucleus. After a long time compared to the natural nuclear time (10^{-21}

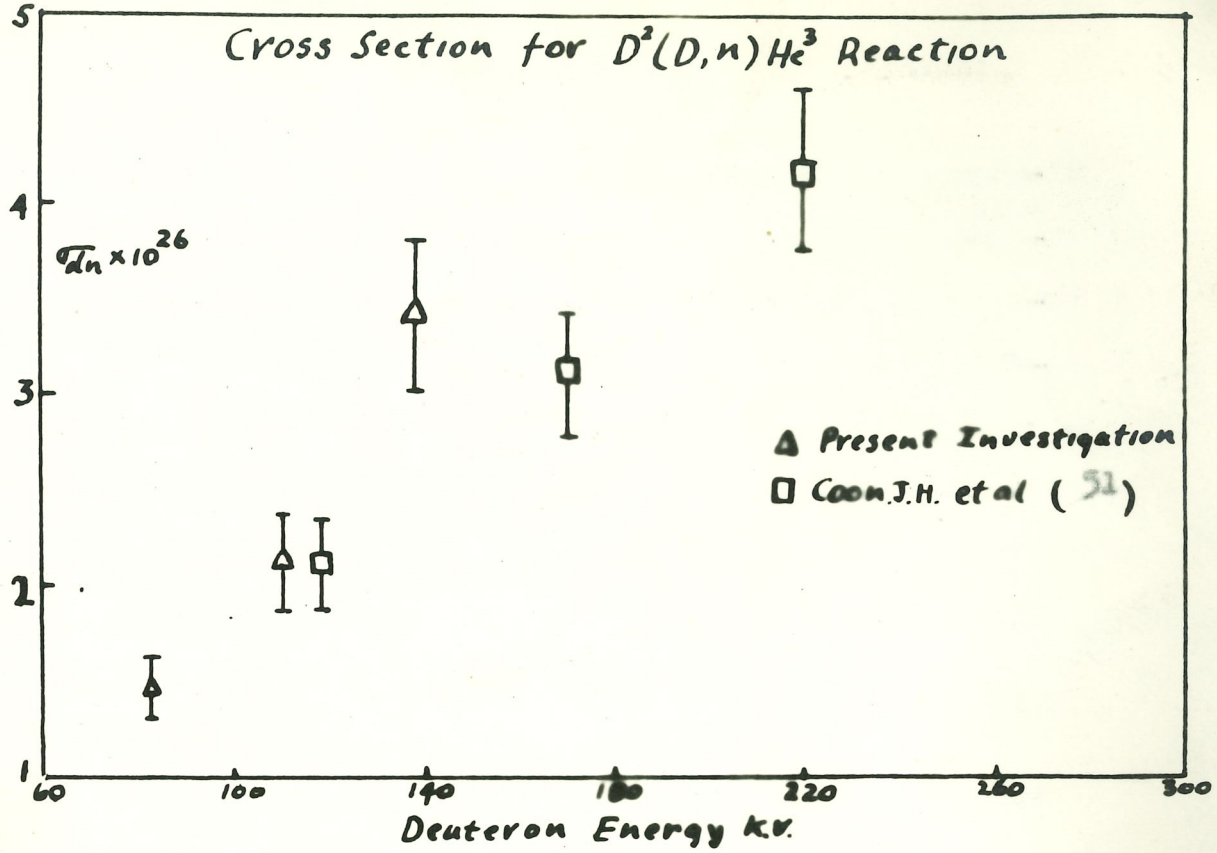


Figure 16.

seconds) this energy is again concentrated on one particle which is expelled. The final break up of the nucleus is thus independent of its mode of formation.

The case of the D-D reaction on this basis can be written:

$$D^2 + D^2 \rightarrow {}^*He^4 \rightarrow H^3 + H^1$$
$$\rightarrow He^3 + n^1$$

Such an excited state of the He^4 nucleus must be a virtual state as it lies a long way above the height of the potential barrier (68). The existence of such a compound nucleus could be inferred from observation on the scattering of neutrons by

He^3 or protons by H^3 (69).

Since the compound nucleus expels either a neutron or a proton and the escape of either is equally probable (proton has sufficient energy to go over top of barrier) the symmetry of nuclear forces requires the probability of the two reactions to be nearly equal and independent of the bombarding energy. Experimentally the branching ratio $\frac{\sigma_{dn}}{\sigma_{dp}}$ is found to increase with energy and this is difficult to explain on the conventional compound nucleus model. The $^*He^4$ nucleus should be able to be formed according to the reaction :

$$n^1 + He^3 \rightarrow {}^*He^4 \rightarrow H^3 + H^1$$
$$\rightarrow D^2 + D^2$$
$$\rightarrow n^1 + He^3$$

No evidence has been found for an unstable level in the compound He^4 nucleus formed by the first reaction using neutron energies up to 0.1 eV. (70). Extension to neutron energies up to 2.5 MeV. is necessary before it can be decided whether a virtual excited level of He^4 exists. It is concluded that the compound nucleus model is as yet inadequate to explain the most important aspects of the D-D reaction.

The Oppenheimer - Phillips Process.

This process has been applied by Peaslee (71) with some success to reactions of deuterons with heavy nuclei. He sets out to explain the general features of proton and neutron

emission in terms of a stripping process, i.e. the incident deuteron is not absorbed directly into the nucleus but either a neutron or a proton is caught by the heavy nucleus without the other deuteron partner coming under the influence of its nuclear field. Two cases are considered :

a) The internal motion of the deuteron is fast compared to the time to pass through the field of the heavy nucleus and polarisation can take place. This process would favour greater proton emission.

b) The internal motion of the deuteron is slow compared to the time which the deuteron is within the range of the heavy nuclei. Case of no polarisation. It is the second case which is found to be most satisfactory.

For the D-D reaction at low bombarding energies neutron transfer from one deuteron to the other results in proton emission. The transfer of a proton is opposed by the Coulomb barrier. When the incident deuteron can surmount the barrier this factor is no longer important. One can expect the ratio $\frac{\sigma dn}{\sigma dp}$ has to increase steadily until the barrier height is reached when $\frac{\sigma dn}{\sigma dp} \simeq 1$. Above this energy the ratio depends on the relative "sticking" probability of the neutron or proton in a deuteron nucleus.

This attempt at an explanation of the qualitative features of the D-D branching ratio is certainly a naive one. Investigations on the assymmetric angular distribution of the reaction products at low energies (72) indicate that an appreciable

contribution to total penetration probability must arise from P waves ($\ell = 1$) otherwise the assymmetry would vanish at low energies. Until additional information on angular distribution and branching ratio is available over a much wider energy range, speculation on the mechanism of the D-D reaction must remain inconclusive.

Conclusion.

It has been demonstrated that the branching ratio of the D-D reaction can be determined by the direct method of measuring the number of He^3 nuclei emitted simultaneously with neutrons.

At low bombarding energies where the yield is small a solid target may be used and no difficulties can be foreseen in extending the measurements down to 15 K.V.

At energies greater than 100 K.V. scattered deuterons caused interference but because of the greatly increased cross section a gas target can be used and the ratio followed up to any desired energy. A knowledge of the branching ratio permits a simple method of monitoring the neutron flux without the necessity of comparison with a neutron standard.

Until further measurements both on angular distribution and branching ratio become available over a much wider energy range it is difficult to form any definite picture of the disintegration mechanism on which to base a theoretical analysis.

Acknowledgements.

The author wishes to thank Professor Lord Cherwell for extending to him the facilities of the Clarendon Laboratory and for the continued interest and encouragement given in the whole course of this work.

In the development and measurements on the ion source Dr. D. Roaf and Messrs. J.H. Sanders and J. Moffatt played an invaluable part particularly in assisting in the construction of the mass spectrograph. The author is also indebted to Mr. P.F.D. Shaw for many helpful discussions on the mechanism of atomic hydrogen recombination on surfaces. The nuclear measurements could not have been made without the whole-hearted cooperation of the accelerator group, Messrs. F.V. Price, G. Preston and K.G. McNeill.

Finally the author wishes to acknowledge the financial assistance given to him by the Imperial Chemical Industries Limited during the latter part of these investigations.

APPENDIX I.

The solution of the equation :

$$\frac{d^2r}{dz^2} = \frac{1}{r}V\left(\frac{I_1}{\dot{z}_1} + \frac{I_2}{\dot{z}_2} + \frac{I_3}{\dot{z}_3}\right) \qquad \text{.... 1.}$$

with the boundary conditions $\frac{dr}{dz} = 0$, $z = 0$ when $r = r_0$

Putting :

$$\dot{z}_1 = \sqrt{\frac{2eV}{m_1}}$$

$$\dot{z}_2 = \sqrt{\frac{2eV}{m_2}} \qquad \text{.... 2.}$$

$$\dot{z}_3 = \sqrt{\frac{2eV}{m_3}}$$

equation 1 becomes :

$$\frac{d^2r}{dz^2} = \frac{1}{r}\left[I_1\sqrt{m_1} + I_2\sqrt{m_2} + I_3\sqrt{m_3}\right]\frac{1}{V^{3/2}\sqrt{2e}} \qquad \text{.... 3.}$$

$$= \frac{k}{r} \qquad \text{where } k \text{ is constant} \qquad \text{.... 3a.}$$

Multiply both sides of 3a. by $2\frac{dr}{dz}$ and integrate giving :

$$\left(\frac{dr}{dz}\right)^2 = 2k\int\frac{1}{r}\frac{dr}{dz}.dz + \text{const} \qquad \text{.... 4.}$$

$$= 2k\log r + \text{const}$$

Putting $\frac{dr}{dz} = 0$ when $r = r_0$ this becomes :

$$\left(\frac{dr}{dz}\right)^2 = 2k\log\frac{r}{r_0} \qquad \text{.... 5.}$$

Equation 5 may be written :

$$\int\frac{dr}{\sqrt{\log\frac{r}{r_0}}} = z\sqrt{2k} + \text{const} \qquad \text{.... 6.}$$

Making a change of variable to $y = \log_e\frac{r}{r_0}$ and $2y\,dy = \frac{dr}{r}$

the left hand side of equation 6 becomes : $\int 2r_0 e y^2\,dy$

and $$2\lambda_0 \int_0^y e^{y^2} dy = z\sqrt{2k}$$ $y = 0$, $z = 0$ when $\lambda = \lambda_0$

Therefore :

$$k = \frac{2}{z^2}\left[\lambda_0 \int_0^y e^{y^2} dy\right]^2 \quad \text{.... 7.}$$

This gives :

$$\left[I_1\sqrt{m_1} + I_2\sqrt{m_2} + I_3\sqrt{m_3}\right]\frac{V^{-3/2}}{\sqrt{2e}} = \frac{2}{z}\left[\lambda_0 \int_0^y e^{y^2} dy\right]^2$$

That is :

$$I_1 = \frac{2\lambda^2}{z^2}\sqrt{\frac{2e}{m_1}}\, V^{3/2}\left[\frac{\lambda_0}{\lambda}\int_0^y e^{y^2} dy\right]^2 - \left(I_2\sqrt{\frac{m_2}{m_1}} + I_3\sqrt{\frac{m_3}{m_1}}\right)$$

APPENDIX II.

Since the original script was written Dr. Roaf has pointed out an additional contribution on the D-D reaction cross sections and angular distribution by Blair et al (73) for incident deuteron energies from 1 to 3.5 MeV. These authors used a single proportional counter for recording all three charged particles from the disintegration and isolated the protons by foils stopping H^3 and He^3 nuclei. It was then necessary to monitor the beam current. Since they demonstrate the equality, in angular distribution, of the two possible reactions the branching ratio at 90° can be computed directly from the total cross sections. A comparison of data over the energy range .086 to 3.5 MeV. is given below :

Energy (MeV).	σ_{an}/σ_{dp}	Reference.
0.086	0.86	Author
0.111	0.94	"
0.119	0.90	(51)
0.139	1.11	Author
0.172	1.13	(51)
0.220	1.32	"
0.300	1.78	"
0.96	1.14	(73)
1.49	1.19	"
2.01	1.17	"
2.51	1.13	"
3.02	1.15	"
3.50	1.13	"

The remarkable constancy of the branching ratio for energies above the Coulomb barrier (420 K.V.) indicates that the "sticking" probability of a neutron or a proton is approximately the same and adds weight to the symmetrical character of nuclear forces.

These results suggest that the branching ratio might be amenable to calculation on the basis of the O-P process for incident energies below the barrier height and simply on the relative sticking probability above the barrier.

REFERENCES.

1. Zinn, W.H.: Phys.Rev., 52, 655, 1937.

2. Scott, G.W.: Phys.Rev., 55, 954, 1939.

3. Finkelnberg, A.T.: Rev.Sci.Inst., 11, 94, 1940.

4. Lamar, E.S.; W.W. Buchner & R.J. van de Graaff: Jour.App. Phys., 12, 132, 1941.

5. Planiol, R.: Comptes Rendus, 204, 1632, 1937.

6. Oliphant, M.L.; & Lord Rutherford: Proc.Roy.Soc., 141, 259, 1933.

7. Penning, F.: Physica, 1191, 1937.

8. Mott, N.F. & H.S.W. Massey, The Theory of Atomic Collisions, Clarendon Press, 1933, p.214.

9. Mott, N.F. & H.S.W. Massey, The Theory of Atomic Collisions, Clarendon Press, 1933, p.179.

10. Bleakney, W.: Phys.Rev., 35, 1180, 1930.

11. Smyth, H.D.: Jour. of Franklin Inst., 198, 795, 1924.

12. Smyth, H.D.: Phys.Rev., 25, 452, 1925.

13. Keene, J.P.: Phil.Mag., 40, 369, 1949.

14. Hersohfelder, J.O.: Jour.Chem.Phys., 6, 795, 1938, & 6, 806, 1938.

15. Hughes, L.L. & A.M. Skellet : Phys.Rev., 30, 11, 1927.

16. Glocker.G. W.Baxter & R Dalton: Jour.Amer.Chem.Soc., 49, 58, 1927.

17. Whiddington, R. & H. Jones : Phil.Mag., 6, 889, 1928.

18. Heitler, W . & F. London : Zeits.f.Physik, 44, 455, 1937.

19. Massey, H.S.W. & C.B.O. Mohr : Proc.Roy.Soc., A135, 258,1937.

20. Hertzberg, G.: Ann.d.Physik, 84, 565, 1927.

21. Wood, R.W.: Proc.Roy.Soc., 102, 1, 1922.

22. Boehm, K.,& F. Bonhaeffer : Zeits.Physik Chem., 119, 385,1926.

23. Poole, H.H. : Proc.Roy.Soc., A163, 404, 1937.

24. Wartenberg, H.v. & H.Schultze : Z.s.f.Phys.Chem., 86, 261, 1930.

25. Pietsch, E. : Zeits.f.Electrochem., 39, Disc.586, 577, 1933.

26. Hiedmann, E. : Zeits.f.Phys.Chem., 164, 1-2, 20, 1933.

27. Gregg, S.J. : The adsorbtion of gases by solids, Methuen Monograph, 1934.

28. Polanyi,M. : Zeits.Elek., 35, 561, 1924

29. Langmuir, I. : Gen.Elect.Rev., 26, 731, 1923.

30. Langmuir, I. & H. Mott-Smith,: Gen.Elect.Rev., 27, p.449, 538, 616, 762, 810, 1924.

31. Mott-Smith, H. & I. Langmuir : Phys.Rev., 28, 727, 1926.

32. Fonks, L. & I. Langmuir : Phys.Rev., 34, 876, 1929.

33. Killian, T.J.: Phys.Rev., 35, 1238, 1930.

34. Schottky, W.: Physik Zeits, 25, 342, 635, 1924.

35. Schottky, W. & Z. Issendorf : Zeits.f.Physik, 31, 163, 1935.

36. Engel, A.v. & M. Steenbeck : Elektrische Gasentladungen, Julius Springer Band 2, p.86, 1934.

37. Engel, A.v. & M. Steenbeck : Elektrische Gasentladungen, Julius Springer Band 1, p.51, 1934.

38. Mott, N.F. & H.S.W. Massey : Theory of Atomic Collisions, Clarendon Press, p.244, 1933.

39. Smyth, H.D. : Atomic Energy for Military Purposes, Rev.Mod. Phys., 17, 438, 1945.

40. Bernas, R.H. & A.O. Nier : Rev.Sci.Inst., 19, 895, 1948.

41. Terman, F. : Radio Engineers Handbook, McGraw-Hill p.337, 1934.

42. Pierce, R. : Jour.App.Phys., 11, 548, 1940.

43. Samuels, A.L. : Proc.I.R.E., 33, 233 , 1945.

44. Field, L.M. : Rev.Mod.Phys., 18, 353, 1946.

45. Thonemann, P.C. : Nature, July 1946.

46. Thompson, J.J. : Phil.Mag., 4, 1128, 1927.

47. Graham, R.C., & A.L. Harkness & H.G. Thode : Jour.Sci.Inst., 24, 119, 1947.

48. Bonner, T.W. & W. Brubaker,: Phys.Rev., 49, 19, 1936.

49. Oliphant, M.L.E., A.E. Kempton & Lord Rutherford : Proc.Roy. Soc., 149, 406, 1935.

50. Dee, P.I. & C.W. Gilbert : Proc.Roy.Soc., 149, 200, 1935.

51. Coon, J.H., R.W. Davies, A.C. Graves, E.R. Graves & J.H. Manley, Report MDDC.206,207.

52. Livingston, M.S. & H.A. Bethe : Rev.Mod.Phys., 9, 261, 1937.

53. Engel, A.v. & M. Steenbeck : Elektrische Gasentladungen, Julius Springer Band 1, 1934.

54. Roberts, A.: Rev.Sci.Inst., 11, 44, 1940.

55. Wilson, H.A. : Modern Physics, Blackie & Son, p.215, 1937.

56. Rice, O.K. : Electron Structure & Chemical Binding, McGraw-Hill, p.329, 1940.

57. Goldsmith, H.H., H.W. Ibser & B.T. Feld : Neutron Cross-Sections of the Elements, Addison-Wesley Press, 1948.

58. Bonner, T.W., J.E. Evans, J.C. Harris & G.C. Philips : Phys.Rev., 75, 1401, 1949.

59. Bethe, H.A. : Ann.d.Physik, 5, 325, 1930.

60. Mott, N.F. : Proc.Cam.Phil.Soc., 27, 553, 1931.

61. Bretscher, E.,A.French & F. Seidl : Phys.Rev., 73, 815, 1948.

62. Bennett, W.E., C. Mandeville & H.T. Richards : Phys.Rev., 69, 418, 1946.

63. Rudnick, P. : Phys.Rev., 38, 1342, 1931.

64. Dolch, H. : Zeits.f.Physik, 100, 401, 1936.

65. Schiff, L.T. : Phys.Rev., 51, 783, 1937.

66. Flugge, S. : Zeits.f.Physik, 108, 545, 1938.

67. Myers, R.D. : Phys.Rev., 54, 361, 1938.

68. Goldstein, L. : Declassified Los Alamos Report No.539, December 1947.

69. Bohr, N. : Nature, p.344, 1936.

70. King, L.D.P. & L. Goldstein : Phys.Rev., 75, 1366, 1949.

71. Peaslee, D.C. : Phys.Rev., 74, 1001, 1948.

72. Konopinski, E.J. & E. Teller : Phys.Rev., 73, 822, 1948.

73. Blair, J.M., G. Freier, G. Lampi, W. Sleater & J.H. Williams, Phys.Rev., 74, 1599, 1948.